EXTERNALIZED GLYCOLYTIC ENZYMES ARE NOVEL, CONSERVED, AND EARLY BIOMARKERS OF APOPTOSIS.

David S. Ucker[1,4], **Mohit Raja Jain[2,3]**, **Goutham Pattabiraman[1]**, **Karol Palasiewicz[1]**,
Raymond B. Birge[3], and **Hong Li[2,3,4]**

[1]Department of Microbiology and Immunology, University of Illinois College of Medicine, Chicago, IL 60612

[2]Center for Advanced Proteomics Research and [3]Department of Biochemistry and Molecular Biology, UMDNJ-New Jersey Medical School Cancer Center, Newark, New Jersey 07214

Running title: Apoptosis-specific externalization of glycolytic enzymes

[4]to whom correspondence should be addressed: David S. Ucker, Department of Microbiology and Immunology (MC 790), University of Illinois College of Medicine, 835 South Wolcott, Chicago, IL 60612, 312 413 1102 (Voice), 312 413 7385 (Fax); DUCK@UIC.EDU (E-MAIL); Hong Li, Department of Biochemistry and Molecular Biology, UMDNJ-NJMS, 205 S. Orange Ave. CC F1226, Newark, NJ 07103, 973 972 8396 (Voice), 973 972 1865 (Fax), LIHO2@UMDNJ.EDU (E-MAIL)

Background: Apoptotic cell recognition triggers profound immunosuppressive responses; relevant recognition determinants are uncharacterized.
Results: Surface exposure of glycolytic enzymes is a common, early apoptotic event.
Conclusion: Externalized glycolytic enzyme molecules are novel apoptotic biomarkers and candidate recognition determinants.
Significance: Apoptotic glycolytic enzyme externalization explicates plasminogen binding to mammalian cells, and potential mechanisms of immune privilege by commensal bacteria and pathogens.

SUMMARY

The intriguing cell biology of apoptotic cell death results in the externalization of numerous autoantigens on the apoptotic cell surface, including protein determinants for specific recognition, linked to immune responses. Apoptotic cells are recognized by phagocytes and trigger an active immunosuppressive response ("innate apoptotic immunity" [IAI]) even in the absence of engulfment. IAI is responsible for the lack of inflammation associated normally with the clearance of apoptotic cells; its failure also has been linked to inflammatory and autoimmune pathology, including systemic lupus erythematosis (SLE) and rheumatic diseases. Apoptotic recognition determinants underlying IAI have yet to be identified definitively; we argue that these molecules are s̲urface-exposed (during apoptotic cell death), u̲biquitously-expressed, p̲rotease-sensitive, e̲volutionarily-conserved, and r̲esident normally in viable cells ("SUPER"). Taking independent and unbiased quantitative proteomic approaches to characterize apoptotic cell surface proteins and identify candidate SUPER determinants, we made the surprising discovery that components of the glycolysis pathway are enriched on the apoptotic cell surface. Our data demonstrate that glycolytic enzyme externalization is a common and early aspect of cell death in different cell types triggered to die with distinct suicidal stimuli. Exposed glycolytic enzyme molecules meet the criteria for IAI-associated SUPER determinants. In addition, our characterization of the apoptosis-specific externalization of glycolytic enzyme molecules may provide insight into the significance of previously reported cases of plasminogen binding to α-enolase on mammalian cells, as well as mechanisms by which commensal bacteria and pathogens maintain immune privilege.

Apoptosis is the primary mechanism by which cells die physiologically and is ongoing throughout life in multi-cellular organisms. A surprising array of cellular components comprising autoantigens are exposed on the surface of apoptotic cells (1). Apoptotic cells are cleared rapidly *in vivo*; that this phagocytic clearance occurs in the absence of inflammation has long been recognized (2). The clearance of apoptotic cells is a key homeostatic process, and represents a final step of the physiological cell death program (3,4). The failure to promptly clear apoptotic cells even has been linked to chronic inflammation and autoimmunity characteristic of systemic lupus erythematosis (SLE), rheumatoid arthritis, and other pathologies including atherosclerosis (5-8). Independent of phagocytosis, specific apoptotic recognition elicits a profound repertoire of affirmative signaling and effector responses in macrophages and neighboring cells associated generally with the suppression of inflammation and immune responsiveness; we have termed this "innate apoptotic immunity" (IAI; refs. 4,9,10). It may be that the autoimmune pathologies observed in association with the persistence of apoptotic

corpses are consequences of deficits in recognition-specific non-phagocytic responses (11).

The anti-inflammatory effects elicited upon the specific recognition of apoptotic cells (12) result primarily from the triggering of transcriptional responses (especially the repression of inflammatory cytokine gene expression) in cells (both professional and non-professional phagocytes) that interact with them (10,13). Subsequent responses, including the production of anti-inflammatory cytokines (e.g. TGF-β, IL-10), extend and may enhance the anti-inflammatory state (14). While numerous molecules have been implicated in the process of apoptotic cells clearance (15), the critical determinants involved in the recognition of apoptotic cells and in the triggering of functional responses to them remain undefined. Our studies have demonstrated that these determinants are evolutionarily conserved and become membrane-exposed during the process of apoptotic cell death without a requirement for ensuing new gene expression (10,13). Here, we add to this characterization and show that they are protease-sensitive. We note that determinants for apoptotic immune recognition and for the phagocytosis of apoptotic cells may not be identical; phosphatidylserine, for example, has been implicated functionally in engulfment (16) and not in innate apoptotic recognition (12,13).

In an effort to understand the molecular basis for innate immune responses to apoptotic cells, we have taken a comprehensive approach toward the identification of the determinants of apoptotic recognition. We have employed two distinct proteomic approaches, based on two-dimensional electrophoretic separations and on "Isobaric tagging for relative and absolute quantification" (iTRAQ), and we have exploited apoptotic membrane vesicles as an enriched source of apoptotic recognition determinants. From our analyses, we identified a large number of over- and under-represented proteins in apoptotic vesicles. We categorized the identified molecules according to previously assigned molecular functions. Notably, these independent approaches both led to the novel observation that numerous components of the glycolysis pathway are enriched on the apoptotic cell surface. Through cytofluorimetric analyses, we have confirmed the apoptosis-associated surface exposure of glycolytic enzymes. Moreover, we have extended these findings to reveal that externalization of glycolytic enzymes is a common attribute of apoptotic cell death, occurring independently of the particular suicidal stimulus and in a variety of cells of different tissue types and species of origin.

Although we have not completed our evaluation of all externalized glycolytic enzyme molecules as determinants of innate apoptotic responses, it is clear that surface-exposed glycolytic enzyme molecules represent novel, early, and unambiguous markers (biomarkers) of the apoptotic cell death process. Surface exposure of glycolytic enzymes has been noted previously in a variety of enteric bacteria and pathogens, and is responsible for specific plasminogen binding (17-27). This striking commonality of glycolytic enzyme externalization raises the possibility that the exposure of glycolytic enzymes on microorganisms reflects a subversion of innate apoptotic immunity though apoptotic mimicry that facilitates commensalism or pathogenesis. In this light, it may be appropriate to reevaluate the significance of reported plasminogen binding activities of glycolytic enzymes.

EXPERIMENTAL PROCEDURES

Cells and Death Induction: Primary murine splenocytes (from C57BL/6 mice), S49 murine thymoma cells, DO11.10 murine T cell hybridomas, RAW 264.7 murine macrophages, Jurkat human T leukemia cells, and U937 human monocytic (histiocytic) leukemia cells were cultured at 37ºC in a humidified, 5% (v / v) CO_2 atmosphere in RPMI 1640 medium (Mediatech; Herndon, VA) supplemented with heat inactivated fetal bovine serum (FBS, 10% v / v; HyClone Laboratories; Logan, UT), 2 mM L-glutamine, and 50 μM 2-mercaptoethanol. HeLa human cervical carcinoma cells and B2 cells, a transfectant reporter clone of 293T human transformed kidney epithelial cells (13), were grown in DMEM medium with 4.5 g / L of glucose (Mediatech) supplemented with FBS (10% v / v) and 2 mM L-glutamine. Physiological cell death (apoptosis) was induced by treatment of cells with the macromolecular synthesis inhibitor actinomycin D (200 ng / ml, 12 hr., ref. 28), by irradiation (20 mJ / cm^2) with UV-C (254 nm) light, or with staurosporine (1 μM in serum-free medium for 3 hr.). Autophagy was induced by serum starvation with L-canavanine (1 mM) in the presence of the pan-caspase inhibitor Quinolyl-Valyl-Aspartyl-difluorophenoxy methyl ketone (Q-VD-OPh [R&D Systems; Minneapolis, MN]; 10 μM), and was confirmed by the development of LC3-GFP puncta in transfected cells (29). Pathological cell death (necrosis) was triggered by incubation of cells at 56ºC for 10-20 min. (until Trypan Blue uptake indicated compromise of membrane integrity). Iron-depleted medium was prepared by treatment with Chelex 100 resin (BioRad; Hercules, CA) as described (30). In some experiments, apoptotic and viable target cells were

2

digested with trypsin (0.1% [w / v] in PBS, 37°C, 15 min; Sigma, St. Louis, MO) and / or fixed by incubation with formaldehyde (125 mm in PBS, 25 °C, 20 min; Polysciences, Inc., Warrington, PA) as described previously (13).

Vesicles: Plasma membrane vesicles were prepared from HeLa cells as described previously (13). Monolayers of cells, either untreated or induced to die for 4 hr. with actinomycin D (and still adherent), were stimulated to vesiculate by incubation at 37°C in Vesiculation Buffer (10 mM Hepes [pH 7.4], 150 mM NaCl, 2 mM CaCl$_2$, 2 mM DTT, and 25 mM formaldehyde). Supernatants were collected after approximately 2.5 hr. (when abundant small membrane vesicles were apparent in the culture fluid). Non-adherent cells were removed (1,000 × g for 10 min., 4°C) and vesicles were pelleted from the cleared supernatant by centrifugation (30,000 × g, 60 min., 4°C). Cytofluorimetric analysis indicated that vesicles were approximately 0.8 µm in diameter and that the level of contaminating intact cells was less than 1 cell per 100 vesicles. Viable vesicles are comparable in size. Protein content was determined by the Bradford method (BioRad); phospholipid content was quantified by the method of Rouser *et al.* (31).

Cytofluorimetric Analyses: For staining with primary antibodies conjugated to fluorescein isothiocyanate (FITC) or phycoerythrin (PE), or for staining with FITC-conjugated plasminogen (BioMac, Leipzig, German), cells were washed twice with cold PBS containing FBS (1%) before resuspension and staining in the same buffer for 40 min. (at 4°C in the dark) prior to washing and cytofluorimetric analysis. Staining involving unconjugated primary antibodies followed the same procedure and was followed by a second incubation with an appropriate FITC- or PE-conjugated secondary antibody. The vendors of the antibodies and staining reagents used are Abcam (Cambridge, MA), BD Biosciences (San Jose CA), Enzo Life Sciences (Farmingdale, NY), Novus Biologicals (Littleton, CO), and Santa Cruz Biotechnology (Santa Cruz, CA).

The accessibility of phosphatidylserine was revealed by the binding of FITC- or PE-conjugated annexin V (BD Biosciences). Cells that had been washed twice in PBS were resuspended in 100 µl of annexin V binding buffer (10 mM HEPES [pH 7.4], 150 mM NaCl, 2.5 mM CaCl$_2$) and incubated with 5µl of the conjugated annexin V for 40 min in the dark at 25°C. Propidium iodide (PI) and 7-amino actinomycin D (7-AAD) were employed to assess plasma membrane integrity. PI (Ex$_\lambda$ = 488 nm, Em$_\lambda$ = 610 nm) or 7-AAD (Ex$_\lambda$ = 488 nm, Em$_\lambda$ = 647 nm) were added to cells (at final concentrations of 1 µg / ml or 4 µg / ml,

respectively) immediately before cytofluorimetric analysis.

For intracellular staining, cells were washed twice with cold PBS and fixed and permeabilized in a solution of formaldehyde and saponin (4% and 0.1%, respectively, in PBS) for 30 min. (at 4°C in the dark). After fixation, cells were washed twice with PBS buffer containing 0.1% saponin and 1% FBS, and stained in this same buffer.

Cells were analyzed cytofluorimetrically on a FacsCaliber instrument (BD Biosciences). The excitation wavelength (Ex$_\lambda$) in all cases was at 488 nm. The fluorescence emission wavelength (Em$_\lambda$) from fluorescein was collected at 530 ± 15 nm; from PI and PE at 610 nm ± 15 nm, and from 7-AAD at 650 ± 20 nm. Cytofluorimetric data were processed with WinMDI software (Joe Trotter, Scripps Research Institute; La Jolla, CA) or Summit v. 4.3 software (Dako; Carpinteria, CA). Where appropriate, fluorescence data are expressed as a Mean Fluorescence Intensity (MFI). Attributes of cell death, including changes in forward-angle and side-angle light scatter, also were evaluated, as described previously (12).

Transcriptional Modulation: Apoptotic immunosuppressive activity was assessed with respect to NFκB-dependent transcription, utilizing a clone of the B2 reporter cell line (B2.1), as described previously (13).

Protein Identification by Two-Dimensional Gel Electrophoresis (2DE): Vesicles were lysed by sonication in isoelectric focusing rehydration buffer (7 M urea, 2 M thiourea, 4% CHAPS, 100 mM DTT, 0.2% Biolytes (pH 5–8), 0.01% Bromophenol Blue and protease inhibitor). Seventy-five µg of protein in a total of 185 µl of rehydration buffer was applied to 11 cm BioRad ReadyStrip IPG Strips (pH 5–8) for overnight rehydration. First-dimension isoelectric focusing was carried out on a BioRad PROTEAN IEF System for a total focusing time of 75000 VH. After focusing, strips were equilibrated with equilibration buffer I (6 M urea, 0.375 M Tris-HCl, pH 8.8, 2% SDS, 20% glycerol, 2% [w / v] DTT) for 15 min. The strips were further equilibrated with equilibration buffer II (6 M urea, 0.375 M Tris-HCl, pH 8.8, 2% SDS, 20% glycerol, 2.5% [w / v] iodoacetamide) for 15 min and directly applied to a 12.5% isocratic SDS-PAGE gel for second dimension. The resulting gel was then fixed (10% acetic acid and 40% ethanol) for 30 min and stained overnight with SYPRO Ruby. Gels were destained (10% methanol, 7.5% acetic acid) for 60 min. After washing with water, gels were scanned on a 9400 Typhoon Variable Mode Imager (GE Healthcare, Inc.; Piscataway, NJ) using a Green (532) Laser and 610BP30

emission filter. Quantitative analysis of spots on gels was performed by PDQuest (BioRad) and visually confirmed.

Protein spots from SYPRO Ruby- stained gels were picked for protein identification. The gel spots were diced into 1 mm^3 pieces and washed with 30% acetonitrile (ACN) in 50 mM ammonium bicarbonate prior to DTT reduction and iodoacetamide alkylation. Trypsin was used for digestion at 37ºC overnight. The resulting peptides were extracted with 30 μl of 1% trifluoracetic acid followed by desalting with C18 Ziptip (Millipore; Bedford, MA). For the mass spectrometry (MS) analysis, the peptides were mixed with 7 mg / ml α-cyano-4-hydroxy-cinnamic acid matrix (in 60% ACN) in a 1:1 ratio and spotted onto a matrix assisted laser desorption / ionization (MALDI) plate. The peptides were analyzed on a 4800 MALDI TOF / TOF analyzer (Applied Biosystems [ABI]; Framingham, MA). Mass spectra (m / z 880-3,200) were acquired in positive ion reflector mode. The 15 most intense ions were selected for subsequent tandem mass spectrometry (MS / MS) sequencing analysis in 1 kV mode. Protein identification was performed by searching the combined MS and MS / MS spectra against the human NCBI database using a local MASCOT search engine (V. 1.9) on a GPS (V. 3.5, ABI) server. Proteins containing at least two peptides with Confidence Interval values no less than 95% were considered being identified.

Protein Quantification by iTRAQ Analysis: For iTRAQ labeling, proteins from vesicle were extracted in an iTRAQ lysis buffer (1% NP40, 1% Triton X-100, 10 mM HEPES, 500 mM triethylammonium bicarbonate buffer [TEAB]) using probe sonication at 50% duty for 3 cycles of 15 sec. with a 60 sec. incubation in ice cold water between cycles. The lysate was cleared by centrifugation at 16,100 × g for 15 min. The pH of samples was adjusted to 8.0 with 1.0 M TEAB. The iTRAQ labeling procedures were performed according to the manufacturer's instructions as further described (32). Briefly, after reduction with Tris (2-carboxyethyl) phosphine hydrochloride and alkylation with methyl methanethiosulfonate, tryptic digestion of each sample (100 μg) was initiated by the addition of 10 μg of trypsin (Promega, Madison, WI), and each sample was incubated at 37°C overnight. Peptides derived from viable samples were labeled with iTRAQ tags 114 and 115 while the peptides from apoptotic samples were labeled with iTRAQ tags 116 and 117. The labeled samples were then mixed together and fractionated via strong cation exchange and reverse phase chromatography according to a procedure described previously (33). The HPLC eluate was mixed with a matrix

solution (7 mg / ml alpha-cyano-4-hydroxycinnamic acid in 60% ACN, 5 mM of ammonium monobasic phosphate, and internal mass calibrants [50 fmol / μl each of Glu-Fib and ACTH, 18–39]) through a 30 nl mixing tee and directly spotted onto the MALDI plates. The peptides were analyzed on a 4800 Proteomics Analyzer MALDI-TOF-TOF tandem mass spectrometer (ABI) in a data-dependent fashion using job wide interpretation. MS spectra (m / z 800–3,600) were acquired in positive ion reflectron mode with internal mass calibration. A maximum of the fifteen most intense ions (S / N >50) per spot were selected for subsequent MS / MS analysis in 1.0 keV mode. Each spectrum was averaged over 2,000 laser shots.

Protein database search and bioinformatics: TS2Mascot (Matrix Science Inc.; Boston, MA, USA) was used to generate peak lists in mascot generic file (MGF) format from the tandem MS spectra, using following parameters (mass range from 20 to 60 Dalton below precursor, S / N ratio ≥10). The peak lists was submitted for automated search using a local Mascot server (version 2.2) against 20,244 proteins in the SwissProt human protein sequence database downloaded from ftp://ftp.ebi.ac.uk/pub/databases/uniprot/knowledgebase. Following parameters were used for the search; iTRAQ 4plex (K), iTRAQ 4plex (N-terminal) and methylthio (C) as fixed modifications; iTRAQ 4plex (Y) and Oxidation (M) as variable modifications; trypsin as the digestive enzyme with up to two missed cleavages allowed; monoisotopic mass with peptide precursor mass tolerance of 50 ppm; MS / MS ion mass tolerance of 0.3 Da. Scaffold (version 3_03_01, Proteome Software Inc., Portland, OR) was used to filter MS / MS based peptide and protein identifications. Peptide identifications were accepted if they could be established at or greater than 95.0% probability and ≤ 1.0% false discovery rate (FDR) as specified by the Peptide Prophet algorithm (34). Protein identifications were accepted if they could be established at or greater than 95.0% probability and contained at least 1 identified peptide at 95% confidence. Protein probabilities were assigned by the Protein Prophet algorithm (35). Proteins that contained similar peptides and could not be differentiated based on MS / MS analysis alone were grouped to satisfy the principles of parsimony. Peptides were quantified using the centroided iTRAQ reporter ion peak intensity. Protein quantitative values were derived from only uniquely assigned peptides. Protein quantitative ratios were calculated as the median of all relevant peptide ratios for each protein. A Log 2 fold ratio for each protein reported by Scaffold were transformed to

normal relative protein abundance fold ratios in Excel (Microsoft; Redmond, WA, USA). A two tailed t-test was performed using Excel for final statistical evaluation. In addition, only proteins altered in abundance by at least 20% from the viable vesicles were considered significant. For each identified protein, associated gene ontology terms were automatically fetched from European Bioinformatics Institute EBI by Scaffold software and plotted with respect to enrichment.

Enzyme assays: Enolase activity was assessed as the fluoride-inhibitable (36) conversion of 2-phosphoglycerate (2-PGE) to phospho-enolpyruvate (PEP), by a modification of an assay described by Pancholi and Fischetti (20). Intact viable and apoptotic HeLa cells were washed once with $1 \times$ PBS. Graded numbers of cells (ranging from 1×10^6 to 3×10^4) were added to a 200 µl reaction in Enolase Buffer (10 mM $MgCl_2$ in $1 \times$ PBS). Reactions were started with the addition of 2-PGE (to a final concentration of 3 mM). After 4 min. of incubation at 25°C, reactions were terminated by adding 800 µl of Enolase Stop Buffer (10 mM $MgCl_2$, 3 mM NaF in $1 \times$ PBS). Cells were removed by centrifugation (5 min. at $600 \times g$), and PEP in supernatants was quantified spectrophotometrically ($\lambda = 240$ nm). The molar extinction coefficient of PEP at 240 nm is 1.164×10^3. Enolase activity in cell extracts (comparably graded cell equivalents) was assessed similarly. Extracts were prepared from viable and apoptotic HeLa cells by sonication (6×10 sec. @ 60 W; Vibra-cell sonicator; Sonics and Materials; Danbury, CT) after allowing the cells to swell on ice in $0.1 \times$ PBS for 30 min. Enolase activity in cell supernatants was assessed after incubating graded numbers of intact cells (as above) in mock reactions in Enolase Buffer without 2-PGE. After 4 min., cells were removed by centrifugation. 2-PGE then was added to the supernatant, and the 2-PGE-dependent production of PEP was assessed after 4 min. as above.

The determination of glyceraldehyde 3–phosphate dehydrogenase (GAPDH) activity followed a similar set of procedures, and was assessed as the conversion of NAD to NADH dependent on glyceraldehyde 3-phosphate (G3P), by a modification of an assay described by Pancholi and Fischetti (17). In particular, the reaction buffer was adjusted to iso-osmolarity. Graded numbers of intact, washed, apoptotic and viable HeLa cells (ranging from 3×10^5 to 1×10^4) were added to a 200 µl reaction in GAPDH Buffer (60 mM NaCl, 50 mM Na_2HPO_4, 40 mM Triethanolamine, 1 mM NAD, pH8.6). Reactions were started by adding G3P to a final concentration of 2 mM. After 4 min. of incubation at 25°C, reactions were terminated by adding 800 µl of GAPDH Stop Buffer (60 mM NaCl, 50 mM Na_2HPO_4, 40 mM Triethanolamine, pH10.0). Cells were removed by centrifugation, and NADH in supernatants was quantified spectrophotometrically ($\lambda = 340$ nm). The molar extinction coefficient of NADH at 340 nm is 6.22×10^3.

RESULTS

Apoptotic suppressive determinants, enriched in membrane vesicles, are protease-sensitive: We have demonstrated that apoptotic determinants for recognition and immune modulation are evolutionarily conserved and arise on the surface of cells during the process of apoptotic death without a requirement for ensuing new gene expression (10,12). The ability of apoptotic cells to modulate inflammatory responses occurs primarily on the level of transcription (10) and can be assessed reliably with transcriptional reporters that disclose primary inflammatory responses (i.e. transcriptional promoters linked to the firefly luciferase gene and responsive to critical transcriptional activators involved in inflammatory responses, such as NFκB; refs. 10,13). **Figure 1** provides examples of the specific dose-dependent effects of apoptotic cells on a responsive cell line harboring such a transcriptional reporter. B2.1 is a highly responsive clone of stably transfected human HEK 293T reporter cells (13). The results presented show that apoptotic cells repress NFκB-dependent transcription whereas viable cells do not, and recapitulate cytokine responses of those cells (13). Importantly, apoptotic cells of distinct species and tissues of origin (S49 [in **Figure 1A**] is a murine T-lymphocyte cell line, and HeLa [in **Figure 1B**] is a human epithelial cell line) trigger equivalent responses.

Previously, we found that the phospholipid phosphatidylserine is neither a sufficient determinant (12) nor a necessary component.(13) for specific apoptotic recognition and immune modulation. We wondered whether apoptotic immunosuppressive activity involves protein determinants and would therefore be susceptible to proteolytic digestion. Indeed, we found that when apoptotic cells were digested with trypsin, their immunomodulatory activity was lost (**Figure 1A**). Interestingly, we find that upon extended incubation following trypsin digestion, apoptotic cells recover modulatory activity (data not shown). Fixation with formaldehyde after protease treatment precludes this recovery, although apoptotic immunomodulatory activity is stable to fixation with formaldehyde (13). We interpret these results to suggest that apoptotic immunomodulatory determinants are protease-sensitive molecules (or molecular complexes

including essential protein components) that are resident in all cells prior to cell death, and that some fraction of the intracellular stores of the relevant molecules becomes surface-exposed (and susceptible to trypsin digestion) due to apoptosis-specific post-translational modification (PTM). For brevity, the acronym SUPER (surface-exposed during apoptotic cell death, ubiquitously-expressed, protease-sensitive, evolutionarily-conserved, and resident normally in viable cells) serves to emphasize these defining properties of apoptotic determinants for recognition and immune modulation.

We have shown that membrane vesicles prepared from apoptotic cells expose these determinants (13). In fact, assays for specific NFκB-dependent transcriptional suppression as a function of the dose of apoptotic vesicles reveal that apoptotic membrane vesicles are enriched in immunomodulatory determinants, relative to whole apoptotic cells and comparable vesicles prepared from viable cells. As shown in **Figure 1B**, titration of the immunomodulatory activity of intact apoptotic HeLa cells and apoptotic vesicles prepared from them demonstrate that vesicles have approximately 25% of the immunomodulatory activity of whole cells. (The low level at which whole cells contaminate vesicle preparations does not account for this activity.) Given that the surface area of whole cells is about 500-fold greater than that of these vesicles (we estimate the ratio of surface areas as $4 \pi r_c^2 / 4 \pi r_v^2 \cong 500$, where r_c, the radius of an intact HeLa cell, is approximately 9 μm and r_v, the average radius of a vesicle, is 0.4 μm) and that the membrane-associated protein content per nanomole of phospholipid of a vesicle is approximately 30-fold greater than that of a whole cell (4.70 μg protein / nmole phospholipid for intact cells versus 0.15 μg protein / nmole phospholipid for vesicles), we calculate the vesicle enrichment of immunomodulatory protein determinants to be greater than 350-fold (i.e. $0.25 \times 500 \times 30 = 375$).

Proteomic analyses of apoptotic membrane vesicles reveal the membrane association of glycolytic enzyme molecules: The implication that determinants of innate apoptotic immunity necessarily include essential protein components and that membrane vesicles provide an enriched source of those determinants led us to undertake a systematic analysis of the proteome of apoptotic plasma membrane vesicles. We performed a comparative analysis of membrane vesicle proteins prepared from apoptotic and viable cells by two-dimensional gel electrophoresis (2DE; **Figure 2**). After electrophoretic resolution, spots of proteins that were distinctly altered in abundance (over- or under-represented) were excised and subjected to tryptic digestion followed by nanoflow liquid chromatography (LC) and tandem mass spectrometry (MS / MS) analysis.

Interestingly, among the most prominent of the over-represented species we observed were proteins known to be involved as enzymes in the terminal stages of glucose metabolism, including pyruvate kinase (PK; highlighted in blue), α-enolase (EnoA; indicated in magenta), and triosephosphate isomerase (TPI; marked in green). Each of these proteins was identified in multiple gel spots (with distinct pI's), and the abundance of each of the distinct spots was found to be increased among proteins from the apoptotic (relative to viable) membrane vesicles (**Figure 2**). The multiple spots may be indicative of isoforms of each of these proteins harboring PTM's. Notably, apoptosis-associated proteolysis does not appear generally to underlie these modifications; only in the case of TPI (spot 7') is an apoptosis-enriched isoform of distinctly lower apparent molecular weight (presumably due to proteolytic cleavage) evident.

Independently, we undertook a complete, quantitative proteomic characterization of apoptotic and viable membrane vesicles, employing iTRAQ technology, which permits the analysis of less abundant species. Apoptotic and viable vesicle extracts were denatured, alkylated, and labeled with isobaric iTRAQ reagent tags (see Experimental Procedures). Duplicate viable vesicle peptides were labeled with iTRAQ reagent tags 114 and 115 (differential tags of 114 and 115 daltons, resp.); duplicate apoptotic membrane peptides were labeled with iTRAQ tags 116 and 117. Samples then were digested with trypsin, and the labeled peptides were mixed in even ratios and quantified by LC / MS / MS. The relative abundance (enrichment or depletion) of distinct peptides in apoptotic and viable samples was determined by replicate comparisons between the labeled samples. From these data, we identified a total of 564 proteins (**Supplemental Table I**; a graphic representation of this distribution, highlighting selected proteins, is shown in **Figure 3**). **Tables I** and **II** list 56 over- represented and 105 under-represented proteins, respectively, that varied by at least 20% between apoptotic and viable membrane vesicle preparations at an FDR of less than 1%. We have previously established, with known standards, that the analytical coefficient of variance is less than 10%; therefore, changes between apoptotic and viable membrane proteins greater than 20% are reliably significant. Notably, the over-represented population included proteins from all intracellular locales (see below).

With the vesiculation protocol, as many as 8% of the cells in an otherwise untreated control

("viable") cell culture become apoptotic. Thus, we would expect that an idealized candidate SUPER molecule (i.e. a protein that is not associated with viable cell membranes and that is associated specifically with apoptotic cell membranes [and that actually is over-represented *x*-fold among apoptotic cell membrane proteins]) would appear to be enriched among apoptotic vesicle proteins no more than approximately 12-fold (i.e. *x* / .08 *x*). Although the membrane vesicles that we prepared have no ultrastructure and are depleted for non membrane-associated molecules, the non surface-exposed, intra-vesicular contents of viable vesicles may contribute further to a diminution of the apparent enrichment of apoptosis-specific membrane proteins in apoptotic vesicle preparations. Indeed, the maximum enrichment of a protein that we observed among apoptotic vesicles (**Figure 3**) was less than 3-fold.

The inventory of apoptotic membrane proteins: We categorized the identified molecules according to previous descriptions of their major molecular functions (**Figure 4**; see below). Molecules characterized for their catalytic activities involved in metabolism constituted the largest group of over-represented proteins present in apoptotic cell vesicles (15 / 56). Among these, glycolytic enzymes (including aldolase, TPI, phosphoglycerate kinase [PGK], EnoA, and PK) were highly represented, consistent with our 2DE analysis. An example of this enrichment, observed by iTRAQ analysis, is presented for EnoA peptides (**Figure 5**). Indeed, it is striking that almost all members of the glycolytic pathway are enriched among apoptotic cell membranes (see **Figure 3 insert**). Other major classes among the over-represented proteins present in apoptotic vesicles are structural (including cytoskeletal) molecules (14 / 56), those (12 / 56) involved in macromolecular synthesis (especially translation) and processing (including proteases), and molecular chaperones (7 / 56).

Importantly, some of the proteins identified here as enriched among apoptotic vesicles (for example, the actin-associated proteins cofilin and ARP 2/3 [ref. 37], numerous heat shock proteins and other chaperones associated with stress [refs. 38-40]) fulfill expectations derived from other studies. Similarly, the mitochondrial protein cytochrome *c* is known to be released from mitochondria during apoptotic cell death (41,42). It is significant that not all of the vesicle-enriched molecules are membrane-exposed; in particular, we do not detect surface-exposed cytochrome *c* (data not shown).

On the other hand, some proteins expected to be enriched in apoptotic vesicles were not identified in this array. Actin was expected to be

among the apoptotic vesicle proteins (43-45), along with actin-associated and other structural molecules. Histones also were expected to be enriched among apoptotic vesicle proteins, based on previous studies documenting their unique presence on the apoptotic cell surface (1). The observation that vesicles have immunomodulatory activity - like intact apoptotic cells - but lack externalized histones - unlike intact apoptotic cells - allows us to exclude histones definitively as apoptotic recognition determinants. Annexin A1, which has been suggested previously to be involved in apoptotic recognition (46), was relatively depleted in our apoptotic vesicle preparation (only ~70% representation; **Table II**) relative to the viable vesicle preparation. Other proteomic studies also have not found annexin A1 to be present generally among apoptotic membrane proteins (see, for example, ref. 47).

It is most striking that both of the independent proteomic analyses we employed identified the preferential membrane vesicle-association of glycolytic enzymes with apoptotic cell death. Since the issue of surface exposure is a defining criterion with regard to apoptotic determinants for recognition and immune modulation (SUPER) candidates, we sought to evaluate whether glycolytic enzyme molecules are present on the apoptotic cell surface.

Cytofluorimetric confirmation of apoptotic externalization of glycolytic enzyme molecules: We examined independently the preferential enrichment of glycolytic enzyme molecules among apoptotic membrane proteins and tested specifically whether those molecules are exposed on the apoptotic cell surface. We analyzed apoptotic cells for the externalization of three glycolytic enzymes (EnoA, GAPDH, and TPI) by immunofluorescence and cytofluorimetric analyses. We examined a variety of cell types and cell lines (in addition to the HeLa cells used to prepare the membrane vesicles subjected to our protein analyses, we analyzed human and murine epithelial, lymphoid, and myeloid cell lines and primary cells induced to undergo apoptotic death with a variety of suicidal stimuli) for cell death-associated externalization of these proteins.

By immunofluorescence staining analysis, we found that EnoA is displayed generally on the surface of apoptotic, but not viable, cells. An example of these analyses (with primary murine splenocytes) is presented in **Figure 6A**. Completely analogous staining patterns were observed for the two other glycolytic enzymes that were analyzed, GAPDH (**Figure 6B**) and TPI (**Figure 6C**). Thus, glycolytic enzyme molecules not only are enriched among apoptotic membrane proteins, but are exposed specifically on the

apoptotic cell surface. Externalized glycolytic enzyme molecules fulfill the critical criteria for apoptotic determinants of recognition and immune modulation: they are evolutionarily conserved proteins that are resident in all cells ubiquitously, and, while unexposed on the surface of viable cells, are membrane-exposed on apoptotic cells.

We evaluated the extent of glycolytic enzyme molecule externalization by comparing immunofluorescence staining of membrane-intact and permeabilized apoptotic cells. Examples of these analyses are presented in **Figure 7**. Permeabilized viable and apoptotic cells stain identically and homogeneously for EnoA (**Figure 7A**), GAPDH (**Figure 7B**), and TPI (data not shown). The extent of externalization of these molecules ranged from 10 – 50% of the total cellular protein for each species during apoptotic cell death (by comparison of mean fluorescence intensities; see **Figure 7** legend). Importantly, these data indicate that the observed apoptosis-specific externalization of glycolytic enzyme molecules is distinct from a general accessibility to intracellular molecules that would result from plasma membrane compromise. In contrast, the detection of glycolytic enzyme molecules on necrotic cells is not distinguishable from plasma membrane compromise (see next). Our data also demonstrate that there is no net elevation of cellular glycolytic enzyme concentration with apoptosis, but rather a preferential externalization of those molecules.

We explored the kinetics of the appearance of these glycolytic enzyme molecules by examining the earliest apoptotic cells (annexin V^+ 7-AAD$^-$) following brief treatment with staurosporine, a potent inducer of apoptosis (**Figure 8**). Externalized EnoA, GAPDH, and TPI could be found already externalized on these early apoptotic cells. Interestingly, the extent of exposure ranged as high as the levels found on later apoptotic cells. By comparison, neither autophagic or necrotic cells expose glycolytic enzyme molecules (Supplemental Figure 1; note that we examined "early" [annexin V^+ 7-AAD$^-$] necrotic cells [12] to preclude the detection of intracellular glycolytic molecules that become accessible with the loss of membrane integrity), consistent with the notion that the externalization of glycolytic enzyme molecules is a specific attribute of the apoptotic cell death process. Furthermore, we have found that the process of glycolytic enzyme externalization, like apoptosis itself, is caspase-dependent (Supplemental Figure 2)

These staining data involve a variety of mono- and polyclonal antibodies. Although all apoptotic cells react with polyclonal sera specific for the glycolytic enzymes, we have noted differences among apoptotic cell populations with regard to reactivity with glycolytic enzyme-specific monoclonal antibodies (data not shown). Some glycolytic enzyme epitopes appear not to be exposed in some cell lines (although those epitopes are immunologically detectable intracellularly). These data suggest that the process of apoptosis-specific externalization may be constrained conformationally (see next section).

In summary, our data from three independent approaches reveal that the externalization of glycolytic enzyme molecules is a dramatic event that occurs reliably and early during the process of apoptotic cell death, and that the surface-exposed, membrane-associated forms of glycolytic enzyme proteins represent novel and unambiguous apoptosis-specific biomarkers.

Externalized glycolytic enzyme molecules lack enzymatic activity: We have assessed enolase and GAPDH activities in apoptotic and viable cells. While apoptotic cells have elevated levels of apparently externalized activity, accounting for 40 – 50% of the total cellular activity observed in whole cell extracts (**Table III**), virtually all of that externalized activity can be attributed to activity leaking from broken cells. That is, we find equivalent activity in cell supernatants prepared by incubation of cells in reaction mixtures (that are of physiological osmolarity) without substrate. Thus, we have no evidence that the "externalized" activities we observe represent the enzymatic activity of enzyme molecules localized to the cell surface, as opposed to the activities of intracellular enzyme molecules released due to plasma membrane leakage. Indeed, we see similar absolute levels of enolase and GAPDH activities associated with undisrupted cells from untreated cultures (although total cellular activities in apoptotic cultures are 40 – 60% lower than in viable cultures; **Table III**).

We conclude that apoptosis-specific externalized enzyme molecules are not enzymatically active. This conclusion is consistent with our suggestion that the process of apoptosis-specific externalization may be conformationally-constrained (above).

Externalized glycolytic enzyme molecules bind plasminogen: Several of the glycolytic enzyme molecules that we have shown to be externalized with apoptosis (especially EnoA, GAPDH, and PGK) have been implicated previously in the binding of plasminogen (48-53). Elevated plasminogen binding associated with apoptotic cell death also has been described (54). Consistent with these observations, we see robust plasminogen binding to apoptotic cells (**Figure 9A**). Plasminogen binding, like glycolytic enzyme

molecule externalization, is evident on the earliest apoptotic cells (**Figure 9B**).

Pre-binding of plasminogen to apoptotic cells precludes the binding of α-enolase-specific antibodies, indicating that EnoA serves as a plasminogen-binding "receptor" (data not shown), although it appears that EnoA is not the only species responsible for plasminogen binding to apoptotic cells. Conversely, plasminogen binding to the apoptotic cell surface is inhibited competitively with the lysine analogue ε–aminocaproic acid (data not shown), consistent with the characterization of cell surface lysine residues as targets for plasminogen binding (48).

In contrast to the glycolytic enzyme molecules, annexin A2, which also has been implicated as a plasminogen-binding receptor (52), is not exposed preferentially during apoptotic cell death. There is concordance between iTRAQ and cytofluorimetric analyses in this regard (**Figures 3 and 10A**). By comparison, cytofluorimetric analysis revealed the apoptosis-specific externalization of calreticulin (**Figure 10B**), although our iTRAQ analysis did not identify calreticulin among apoptotic membrane vesicle-enriched molecules (**Figure 3**). The exposure of calreticulin in association with apoptotic cell death has been noted previously (55, but see 56).

DISCUSSION

Efficient recognition of the corpse, coupled to immunomodulation, is perhaps the ultimate functional consequence of apoptotic cell death, and the identification of the relevant molecules that determine those outcomes is of fundamental importance. Based on results from a variety of our studies indicating that apoptotic immunomodulatory determinants, which can be evaluated by the transcriptional responses they elicit, appear relatively early in the process of cell death, are enriched in plasma membrane vesicles from apoptotic cells, and are protease sensitive, we undertook distinct, independent, and unbiased proteomic approaches to characterize apoptosis-specific (as compared with viable) membrane vesicle-associated proteins. We elaborated criteria that represent critical features of the molecules that function as apoptotic determinants for recognition and immune response modulation (denoted "SUPER"): molecules that become surface-exposed specifically during apoptotic cell death process, that are expressed ubiquitously in cells of different cell types, that are protease-sensitive, evolutionarily-conserved, and that are resident normally in viable cells (albeit not on the cell surface of non-apoptotic cells).

There were intriguing and informative surprises in the array of proteins identified. For example, the absence of histones, which meet the SUPER criteria for apoptotic determinants for recognition and immune modulation, is striking. The absence of histones from apoptotic vesicles may reflect their loose associated with the apoptotic cell membrane and loss as a consequence of the extensive washing and ultracentrifugation involved in vesicle preparation. The apparent absence of actin (as distinct from molecules with which it shares significant sequence identity [e.g. actinin, etc.]) may simply represent an artifact of the informatic paradigm by which protein assignments from identified peptides are made, although, by immunofluorescence staining, we have not detected actin associated with apoptotic vesicles (data not shown). Presumably, the enrichment of cytochrome *c* among apoptotic vesicle proteins reflects the release of soluble cytochrome *c* from mitochondria during the apoptotic process, while the absence of cytochrome c from the cell surface underscores the selectivity of apoptosis-specific protein externalization.

Unexpectedly, we identified a group of glycolytic enzyme molecules that become redistributed and membrane-associated during apoptotic cell death, and we demonstrated cytofluorimetrically their externalization to the apoptotic cell surface. With the exception of two of the upstream members (hexokinase and phosphofructokinase), all of the enzymes of the aerobic glycolytic pathway (phosphoglucose isomerase, aldolase, TPI, GAPDH, PGK, EnoA, and PK) were identified as enriched in the membrane vesicle fraction from apoptotic cells. Previous work (57,58) has documented that glycolytic enzymes are not [normally] associated with the plasma membrane. Still, our results are consistent with findings from other proteomic studies. For example, Gu *et al.* (59) observed that several glycolytic enzymes (including EnoA and glyceraldehyde 3-phosphate dehydrogenase [GAPDH]) were up-regulated at late times of death (triggered by activation of p53), and Jin *et al.* (45) found EnoA and GAPDH in microparticles recovered from human plasma, which include apoptotic blebs. Sunaga *et al.* (60) also noted that GAPDH is over-expressed during the apoptotic death of neuronal cells and that it is exposed in amyloid plaques. Interestingly, thesemolecules have been shown to form multimeric complexes intracellularly on cytoskeletal and membrane elements in viable cells (61-64); we do not know if they exist in an aggregated form when externalized.

Our data demonstrate that glycolytic enzyme molecule externalization is a common and early aspect of apoptotic cell death in different cell types

triggered to die with distinct suicidal stimuli. Although all apoptotic cells expose glycolytic enzyme molecules, only a fraction of those molecules within a cell is externalized to the cell surface; the externalized molecules lack enzymatic activity. Numerous metabolic processes and enzymes have been shown to be important for many aspects of apoptosis (65-68); however, the redistribution of a large subset of glycolytic enzymes to the apoptotic cell membrane has not been characterized previously. Our findings demonstrate that the externalization of glycolytic enzyme molecules is a unique feature and a definitive marker of apoptotic cell death.

GAPDH and EnoA externalization have been noted previously in particular cases. GAPDH, for example, has been reported to serve as a receptor for transferrin (30). Raje *et al.* found that GAPDH was externalized on cells of a macrophage cell line cultured in iron-depleted medium (30). We repeated those experiments (with the same macrophage cell lines and others) and found that the iron-deficient conditions employed trigger apoptotic cell death, leading to the exposure of GAPDH (and other glycolytic enzyme molecules; data not shown). Thus, those findings reiterate that externalized GAPDH is a definitive marker of the apoptotic cell, independent of transferrin-binding activity. The case of plasminogen binding to externalized EnoA is discussed below.

The cohort of externalized glycolytic enzyme molecules that we identified by several approaches fulfill the critical SUPER criteria. Others of the molecules enriched among apoptotic membrane vesicles and identified in our iTRAQ analysis also meet SUPER criteria. Those found not to be externalized (e.g. actin, cytochrome *c*, and histones; discussed above) likely can be excluded from further consideration. In addition, the group of chaperones likely does not function as apoptotic immunosuppressive determinants; heat shock proteins, in particular, have been implicated as immunostimulatory "danger signals" (69).

Further, since exposure of resident, intracellular molecules from necrotic cells does not confer apoptotic-like immunosuppressive activity (10,12), protein externalization *per se* (in the absence of apoptosis-specific PTM) likely is not sufficient for the appearance of apoptotic determinants for recognition and immune modulation. At least with regard to EnoA, our data demonstrating that the appearance of apoptotic determinants for recognition and immune response modulation is not dependent on *de novo* gene expression (10,12) are consistent with the suggestion of Redlitz *et al.* (49) that the surface-exposed form of that molecule does not

arise as the product of a specific or altered gene transcript.

It is not clear how apoptosis-specific protein externalization occurs, although our data indicate that it occurs in a caspase-dependent manner . The externalization of glycolytic enzymes has been observed in a wide variety of cells and among many species, independent of cell death (17-27,48-50,53). Among these examples are bacterial and protist pathogens, some of which have been shown to mimic apoptotic cell immune responses (70,71). The export signals or mechanism by which those normally intracellular molecules become membrane-exposed have not been identified. The enzymatically inactive forms of externalized glycolytic enzyme molecules on apoptotic cells contrast with the enzymatically active glycolytic enzymes exposed on the bacterial surface (17,18,20), suggesting that different processes for membrane externalization may pertain.

As discussed above, we observe similar mobilities (both relative molecular weight and pI; **Figure 2**) for non-externalized glycolytic enzyme molecules that are derived from viable cells, and for the glycolytic enzyme molecules of apoptotic cells, at least a large fraction of which are externalized. With the exception of TPI, where there does appear to be apoptosis-enhanced proteolysis (**Figure 2**, spot 7'), it is clear from these data that apoptosis-specific post-translational modifications that give rise to glycolytic enzyme molecule externalization generally are not proteolytic. Our analysis of such modifications, including the possibility of oxidation-dependent modification (72), is underway. Notably, apoptotic externalization appears to target proteins selectively and independently of protein abundance. The process of blebbing (73-76), which is characteristic of apoptosis, involves protein relocalization (1). We do not know whether blebbing *per se* is sufficient for the protein externalization that we have characterized.

Externalization of EnoA has been noted in the context of its ability to bind plasminogen (48-51). The nature of the cells exposing EnoA on the cell surface was not explored in those studies. Our data show that significant binding of plasminogen occurs specifically to apoptotic (and not viable) cells, and that EnoA is involved in [at least some of] this binding. These results confirm and extend previous observations (54). In particular, independent studies have implicated externalized glycolytic enzymes (especially EnoA and GAPDH) on mammalian and pathogen surfaces as sites for plasminogen binding and activation (18,27,77,78), although no compelling physiological rationale for the presence of this activity on such disparate cells has been offered.

Plasminogen binding, leading to proteolytic cleavage and plasmin activation, has been suggested to be important for pathogen invasiveness (27,79). With mammalian cells, several, but not all, species of plasminogen receptor molecules are enriched on the surface of apoptotic cells. It seems unlikely that migration and invasiveness (e.g. extracellular matrix degradation) are selected attributes for apoptotic cells, although plasmin-dependent proteolytic activation of latent, matrix-associated TGF-β may be significant (see ref. 80). Plasminogen also appears to be a component of serum that enhances phagocytosis of apoptotic cells (K. Lauber, personal communication). Although molecules identified as plasminogen receptors that are externalized in a non-cell death-related manner, such as annexin A2, may be physiologically relevant for plasminogen binding and its consequences (81,82), plasminogen-binding molecules exposed in an apoptosis-specific manner may function in an entirely distinct capacity on the apoptotic cell surface.

Several molecular species of "plasminogen receptors" other than glycolytic enzyme molecules have been identified. For example, Das and Plow (83,84) have suggested that histone H2B is a plasminogen receptor, and cell surface actin has been implicated similarly (44,52,85). In this context, it is interesting that our iTRAQ analysis indicates that these and other molecules characterized as (or associated with) plasminogen receptors (S100A10, annexin A2, cytokeratin 8; refs. 82,86,87) are not preferentially enriched on the apoptotic cell surface (**Figure 3**).

We take our data to suggest that plasminogen binding *per se* may not represent the primary functional consequence of apoptosis-specific protein externalization; rather, the externalization of glycolytic enzyme molecules may be significant functionally in apoptotic cell recognition and immune modulation. In this context, the significance of the expression of orthologous molecules on bacterial (and other pathogenic) surfaces may relate to apoptotic mimicry, leading to immune suppression (attenuation of inflammatory and other immune responses), rather than to plasminogen binding. Our results, then, may serve to integrate diverse previous findings to suggest that the observed binding of plasminogen to glycolytic enzyme molecules exposed on the mammalian cell surface is a consequence of the apoptosis-specific externalization of determinants for recognition and immune modulation, and that apoptotic mimicry is the primary effect of exposed glycolytic molecules on commensal bacterial and pathogens.

Independently of their intracellular roles in metabolism (as well as more recently identified functions in transcription, cytoskeletal trafficking, and autophagy and cell death; refs. 88-92), our findings proffer glycolytic enzyme molecules, in an extracellular context, as candidate determinants of immunomodulation and suggest that they may fulfill an immunological "moonlighting" (93) role. It is not surprising that in cases of autoimmune pathology, where normal innate apoptotic immunity and tolerance is broken, these molecules are recognized as autoantigens to which antibodies are generated. Indeed, glycolytic enzymes have been identified as potent autoantigens in several autoimmune syndromes (e.g. EnoA in Hashimoto's encephalopathy, Behçet's disease, SLE, inflammatory bowel disease, vasculitis, mixed cryoglobulinemia, and rheumatoid arthritis; refs. 94-100; TPI in neuropsychiatric lupus, SLE, and osteoarthritis; refs. 101,102; PK in rheumatoid arthritis as well as SLE; ref. 103). Further characterization of the apoptosis-specific mechanism by which glycolytic enzymes are post-translationally modified and externalized and their role in immune modulation holds promise for understanding and addressing causes of autoimmune and inflammatory pathology.

REFERENCES

1. Cocca, B. A., Cline, A. M., and Radic, M. Z. (2002) *J. Immunol.* **169**, 159-166
2. Kerr, J. F. R., Wyllie, A. H., and Currie, A. R. (1972) *Br. J. Cancer* **26**, 239-256
3. Savill, J., Dransfield, I., Gregory, C., and Haslett, C. (2002) *Nat. Rev. Immunol.* **2**, 965-975
4. Birge, R. B., and Ucker, D. S. (2008) *Cell Death Differ.* **15**(7), 1096-1102
5. Herrmann, M., Voll, R. E., Zoller, O. M., Hagenhofer, M., Ponner, B. B., and Kalden, J. R. (1998) *Arthritis Rheum.* **41**, 1241-1250
6. Cohen, P. L., Caricchio, R., Abraham, V., Camenisch, T. D., Jennette, J. C., Roubey, R. A. S., Earp, H. S., Matsushima, G., and Reap, E. A. (2002) *J. Exp. Med.* **196**, 135-140
7. Rothlin, C. V., Ghosh, S., Zuniga, E. I., Oldstone, M. B., and Lemke, G. (2007) *Cell* **131**(6), 1124-1136
8. Thorp, E. B. (2010) *Apoptosis* **15**(9), 1124-1136
9. Ucker, D. S. (2009) Innate apoptotic immunity: a potent immunosuppressive response repertoire elicited by specific apoptotic cell recognition. In: Krysko, D. V., and Vandenabeele, P. (eds).

Phagocytosis of dying cells: from molecular mechanisms to human diseases, Springer, Berlin, New York

10. Cvetanovic, M., and Ucker, D. S. (2004) *J. Immunol.* **172**, 880-889
11. Patel, V. A., Longacre-Antoni, A., Cvetanovic, M., Lee, D. J., Feng, L., Fan, H., Rauch, J., Ucker, D. S., and Levine, J. S. (2007) *Autoimmunity* **40**(4), 274-280
12. Cocco, R. E., and Ucker, D. S. (2001) *Mol. Biol. Cell* **12**(4), 919-930
13. Cvetanovic, M., Mitchell, J. E., Patel, V., Avner, B. S., Su, Y., van der Saag, P. T., Witte, P. L., Fiore, S., Levine, J. S., and Ucker, D. S. (2006) *J. Biol. Chem.* **281**, 20055-20067
14. Fadok, V. A., Bratton, D. L., Konowal, A., Freed, P. W., Westcott, J. Y., and Henson, P. M. (1998) *J. Clin. Invest.* **101**, 890-898
15. Savill, J. (1998) *Nature* **392**, 442-443
16. Fadok, V. A., Voelker, D. R., Campbell, P. A., Cohen, J. J., Bratton, D. L., and Henson, P. M. (1992) *J. Immunol.* **148**, 2207-2216
17. Pancholi, V., and Fischetti, V. A. (1992) *J. Exp. Med.* **176**(2), 415-426
18. Bergmann, S., Rohde, M., Chhatwal, G. S., and Hammerschmidt, S. (2001) *Mol. Microbiol.* **40**(6), 1273-1287
19. Bergmann, S., Rohde, M., and Hammerschmidt, S. (2004) *Infect. Immun.* **72**(4), 2416-2419
20. Pancholi, V., and Fischetti, V. A. (1998) *J. Biol. Chem.* **273**(23), 14503-14515
21. Candela, M., Biagi, E., Centanni, M., Turroni, S., Vici, M., Musiani, F., Vitali, B., Bergmann, S., Hammerschmidt, S., and Brigidi, P. (2009) *Microbiology* **155**(Pt 10), 3294-3303
22. Vanegas, G., Quinones, W., Carrasco-Lopez, C., Concepcion, J. L., Albericio, F., and Avilan, L. (2007) *Parasitol. Res.* **101**(6), 1511-1516
23. Lama, A., Kucknoor, A., Mundodi, V., and Alderete, J. F. (2009) *Infect. Immun.* **77**(7), 2703-2711
24. Bhowmick, I. P., Kumar, N., Sharma, S., Coppens, I., and Jarori, G. K. (2009) *Malar. J.* **8**, 179
25. Gil-Navarro, I., Gil, M. L., Casanova, M., O'Connor, J. E., Martinez, J. P., and Gozalbo, D. (1997) *J. Bacteriol.* **179**(16), 4992-4999
26. Goudot-Crozel, V., Caillol, D., Djabali, M., and Dessein, A. J. (1989) *J. Exp. Med.* **170**(6), 2065-2080
27. Jong, A. Y., Chen, S. H. M., Stins, M. F., Kim, K. S., Tuan, T.-L., and Huang, S.-H. (2003) *J. Med. Microbiol.* **52**(Pt 8), 615-622
28. Chang, S. H., Cvetanovic, M., Harvey, K. J., Komoriya, A., Packard, B. Z., and Ucker, D. S. (2002) *Exp. Cell Res.* **277**, 15-30
29. Kabeya, Y., Mizushima, N., Ueno, T., Yamamoto, A., Kirisako, T., Noda, T., Kominami, E., Ohsumi, Y., and Yoshimori, T. (2000) *EMBO J.* **19**(21), 5720-5828
30. Raje, C. I., Kumar, S., Harle, A., Nanda, J. S., and Raje, M. (2007) *J. Biol. Chem.* **282**(5), 3252-3261
31. Rouser, G., Fleischer, S., and Yamamoto, A. (1970) *Lipids* **5**(5), 494-496
32. Jain, M. R., Bian, S., Liu, T., Hu, J., Elkabes, S., and Li, H. (2009) *Proteome Sci.* **7**, 25
33. Jain, M. R., Liu, T., Hu, J., Darfler, M., Fitzhugh, V., Rinaggio, J., and Li, H. (2008) *Open Proteomics J.* **1**, 40-45
34. Keller, A., Nesvizhskii, A. I., Kolker, E., and Aebersold, R. (2002) *Anal. Chem.* **74**(20), 5383-5392
35. Nesvizhskii, A. I., Keller, A., Kolker, E., and Aebersold, R. (2003) *Anal. Chem.* **75**(17), 4646-4658
36. Kanapka, J. A., and Hamilton, I. R. (1971) *Arch. Biochem. Biophys.* **146**(1), 167-174
37. Mannherz, H. G., Gonsior, S. M., Gremm, D., Wu, X., Pope, B. J., and Weeds, A. G. (2005) *Eur. J. Cell Biol.* **84**(4), 503-515
38. Buttyan, R., Zakeri, Z., Lockshin, R., and Wolgemuth, D. (1988) *Mol. Endocrinol.* **2**, 650-657
39. Zinszner, H., Kuroda, M., Wang, X. Z., Batchvarova, N., Lightfoot, R. T., Remotti, H., Stevens, J. L., and Ron, D. (1998) *Genes Devel.* **12**, 982-995
40. Huot, J., Houle, F., Rousseau, S., Deschesnes, R. G., Shah, G. M., and Landry, J. (1998) *J. Cell Biol.* **143**(5), 1361-1373
41. Kluck, R. M., Bossy-Wetzel, E., Green, D. R., and Newmeyer, D. D. (1997) *Science* **275**, 1132-1136
42. D'Herde, K., De Prest, B., Mussche, S., Schotte, P., Beyaert, R., Van Coster, R., and Roels, F. (2000) *Cell Death Differ.* **7**, 331-337
43. Laster, S. M., and Mackenzie, J. M., Jr. (1996) *Microsc. Res. Tech.* **34**, 272-280

44. Dudani, A. K., and Ganz, P. R. (1996) *Br. J. Haematol.* **95**(1), 168-178
45. Jin, M., Drwal, G., Bourgeois, T., Saltz, J., and Wu, H. M. (2005) *Proteomics* **5**(7), 1940-1952
46. Arur, S., Uche, U. E., Rezaul, K., Fong, M., Scranton, V., Cowan, A. E., Mohler, W., and Han, D. K. (2003) *Dev. Cell* **4**, 587-598
47. Miguet, L., Pacaud, K., Felden, C., Hugel, B., Martinez, M. C., Freyssinet, J. M., Herbrecht, R., Potier, N., van Dorsselaer, A., and Mauvieux, L. (2006) *Proteomics* **6**(1), 153-171
48. Miles, L. A., Dahlberg, C. M., Plescia, J., Felez, J., Kato, K., and Plow, E. F. (1991) *Biochemistry* **30**, 1682-16891
49. Redlitz, A., Fowler, B. J., Plow, E. F., and Miles, L. A. (1995) *Eur. J. Biochem.* **227**(1-2), 407-415
50. Nakajima, K., Hamanoue, M., Takemoto, N., Hattori, T., Kato, K., and Kohsaka, S. (1994) *J. Neurochem.* **63**(6), 2048-2057
51. López-Alemany, R., Suelves, M., and Muñoz-Cánoves, P. (2003) *Thromb. Haemost.* **90**(4), 724-733
52. Kwon, M., MacLeod, T. J., Zhang, Y., and Waisman, D. M. (2005) *Front. Biosci.* **10**, 300-325
53. Wygrecka, M., Marsh, L. M., Morty, R. E., Henneke, I., Guenther, A., Lohmeyer, J., Markart, P., and Preissner, K. T. (2009) *Blood* **113**(22), 5588-5598
54. O'Mullane, M. J., and Baker, M. S. (1998) *Exp. Cell Res.* **242**(1), 153-164
55. Obeid, M., Tesniere, A., Ghiringhelli, F., Fimia, G. M., Apetoh, L., Perfettini, J.-L., Castedo, M., Mignot, G., Panaretakis, T., Casares, N., Métivier, D., Larochette, N., van Endert, P., Ciccosanti, F., Piacentini, M., Zitvogel, L., and Kroemer, G. (2007) *Nat. Med.* **13**(1), 54-61
56. Gardai, S. J., McPhillips, K. A., Frasch, S. C., Janssen, W. J., Starefeldt, A., Murphy-Ullrich, J. E., Bratton, D. L., Oldenborg, P. A., Michalak, M., and Henson, P. M. (2005) *Cell* **123**, 321-334
57. Shui, W., Sheu, L., Liu, J., Smart, B., Petzold, C. J., Hsieh, T. Y., Pitcher, A., Keasling, J. D., and Bertozzi, C. R. (2008) *Proc. Natl. Acad. Sci. USA* **105**(44), 16952-16957
58. Rogers, L. D., and Foster, L. J. (2007) *Proc. Natl. Acad. Sci. USA* **104**(47), 18520-18525
59. Gu, S., Liu, Z., Pan, S., Jiang, Z., Lu, H., Amit, O., Bradbury, E. M., Hu, C.-A. A., and Chen, X. (2004) *Mol. Cell. Proteomics* **3**(10), 998-1008
60. Sunaga, K., Takahashi, H., Chuang, D.-M., and Ishitani, R. (1995) *Neurosci. Lett.* **200**(2), 133-136
61. Srere, P. A., and Knull, H. R. (1998) *Trends Biochem. Sci.* **23**(9), 319-320
62. Singh, P., Salih, M., Leddy, J. J., and Tuana, B. S. (2004) *J. Biol. Chem.* **279**(34), 35176-35182
63. Minaschek, G., Groschel-Stewart, U., Blum, S., and Bereiter-Hahn, J. (1992) *Eur. J. Cell Biol.* **58**(2), 418-428
64. Campanella, M. E., Chu, H., and Low, P. S. (2005) *Proc. Natl. Acad. Sci. USA* **102**(7), 2402-2407
65. Ishitani, R., and Chuang, D.-M. (1996) *Proc. Natl. Acad. Sci. USA* **93**(18), 9937-9941
66. Eguchi, Y., Shimizu, S., and Tsujimoto, Y. (1997) *Cancer Res.* **57**, 1835-1840
67. Leist, M., Single, B., Castoldi, A. F., Kühnle, S., and Nicotera, P. (1997) *J. Exp. Med.* **185**, 1481-1486
68. Robey, R. B., and Hay, N. (2006) *Oncogene* **25**(34), 4683-4696
69. Manjili, M. H., Park, J., Facciponte, J. G., and Subjeck, J. R. (2005) *Immunobiology* **210**(5), 295-303
70. de Freitas Balanco, J. M., Moreira, M. E. C., Bonomo, A., Bozza, P. T., Amarante-Mendes, G., Pirmez, C., and Barcinski, M. A. (2001) *Curr. Biol.* **11**, 1870-1873
71. Barcinski, M. A., Moreira, M. E. C., de Freitas Balanco, J. M., Wanderley, J. L. M., and Bonomo, A. C. (2003) *Kinetoplastid Biol. Dis.* **2**, 6-7
72. Sambrano, G. R., and Steinberg, D. (1995) *Proc. Natl. Acad. Sci. USA* **92**, 1396-1400
73. Mills, J. C., Stone, N. L., Erhardt, J., and Pittman, R. N. (1998) *J. Cell Biol.* **140**, 627-636
74. Coleman, M. L., Sahai, E. A., Yeo, M., Bosch, M., Dewar, A., and Olson, M. F. (2001) *Nat. Cell Biol.* **3**, 339-345
75. Sebbagh, M., Renvoizé, C., Hamelin, J., Riché, N., Bertoglio, J., and Bréard, J. (2001) *Nat. Cell Biol.* **3**, 346-352
76. Leverrier, Y., and Ridley, A. J. (2001) *Nat. Cell Biol.* **3**, E91-E93
77. Felez, J., Chanquia, C. J., Fabregas, P., Plow, E. F., and Miles, L. A. (1993) *Blood* **82**(8), 2433-2441
78. Miles, L. A., Hawley, S. B., Baik, N., Andronicos, N. M., Castellino, F. J., and Parmer, R. J. (2005) *Front. Biosci.* **10**, 1754-1762
79. Lähteenmäki, K., Edelman, S., and Korhonen, T. K. (2005) *Trends Microbiol.* **13**(2), 79-85

80. Plow, E. F., Herren, T., Redlitz, A., Miles, L. A., and Hoover-Plow, J. L. (1995) *FASEB J.* **9**(10), 939-945
81. Odaka, C., Tanioka, M., and Itoh, T. (2005) *J. Immunol.* **174**(2), 846-853
82. Falcone, D. J., Borth, W., Khan, K. M., and Hajjar, K. A. (2001) *Blood* **97**(3), 777-784
83. Das, R., Burke, T., and Plow, E. F. (2007) *Blood* **110**(10), 3763-3772
84. Herren, T., Burke, T. A., Das, R., and Plow, E. F. (2006) *Biochemistry* **45**(31), 9463-9474
85. Hawley, S. B., Green, M. A., and Miles, L. A. (2000) *Thromb. Haemost.* **84**(5), 882-890
86. Ling, Q., Jacovina, A. T., Deora, A., Febbraio, M., Simantov, R., Silverstein, R. L., Hempstead, B., Mark, W. H., and Hajjar, K. A. (2004) *J. Clin. Invest.* **113**(1), 38-48
87. Cesarman, G. M., Guevara, C. A., and Hajjar, K. A. (1994) *J. Biol. Chem.* **269**(33), 21198-22203
88. Feo, S., Arcuri, D., Piddini, E., Passantino, R., and Giallongo, A. (2000) *FEBS Lett.* **473**, 47-52
89. Colell, A., Ricci, J.-E., Tait, S., Milasta, S., Maurer, U., Bouchier-Hayes, L., Fitzgerald, P., Guio-Carrion, A., Waterhouse, N. J., Li, C. W., Mari, B., Barbry, P., Newmeyer, D. D., Beere, H. M., and Green, D. R. (2007) *Cell* **129**(5), 983-997
90. Tisdale, E. J. (2002) *J. Biol. Chem.* **277**(5), 3334-3341
91. Glaser, P. E., Han, X., and Gross, R. W. (2002) *Proc. Natl. Acad. Sci. USA* **99**(22), 14104-14109
92. Tisdale, E. J., Azizi, F., and Artalejo, C. R. (2009) *J. Biol. Chem.* **284**(9), 5876-5884
93. Jeffery, C. J. (2009) *Mol. BioSyst.* **5**(4), 345-350
94. Sabbatini, A., Dolcher, M. P., Marchini, B., Chimenti, D., Moscato, S., Pratesi, F., Bombardieri, S., and Migliorini, P. (1997) *Clin. Exp. Rheumatol.* **15**(6), 655-658
95. Roozendaal, C., Zhao, M. H., Horst, G., Lockwood, C. M., Kleibeuker, J. H., Limburg, P. C., Nelis, G. F., and Kallenberg, C. G. M. (1998) *Clin. Exp. Immunol.* **112**(1), 10-16
96. Pratesi, F., Moscato, S., Sabbatini, A., Chimenti, D., Bombardieri, S., and Migliorini, P. (2000) *J. Rheumatol.* **27**(1), 109-115
97. Moscato, S., Pratesi, F., Sabbatini, A., Chimenti, D., Scavuzzo, M., Passatino, R., Bombardieri, S., Giallongo, A., and Migliorini, P. (2000) *Eur. J. Immunol.* **30**, 3575-3584
98. Saulot, V., Vittecoq, O., Charlionet, R., Fardellone, P., Lange, C., Marvin, L., Machour, N., Le Loët, X., Gilbert, D., and Tron, F. (2002) *Arthritis Rheum.* **46**(5), 1196-1201
99. Lee, K. H., Chung, H.-S., Kim, H. S., Oh, S.-H., Ha, M.-K., Baik, J.-H., Lee, S., and Bang, D. (2003) *Arthritis Rheum.* **48**(7), 2025-2035
100. Fujii, A., Yoneda, M., Ito, T., Yamamura, O., Satomi, S., Higa, H., Kimura, A., Suzuki, M., Yamashita, M., Yuasa, T., Suzuki, H., and Kuriyama, M. (2005) *J. Neuroimmunol.* **162**(1-2), 130-136
101. Xiang, Y., Sekine, T., Nakamura, H., Imajoh-Ohmi, S., Fukuda, H., Nishioka, K., and Kato, T. (2004) *Arthritis Rheum.* **50**(5), 1511-1521
102. Sasajima, T., Watanabe, H., Sato, S., Sato, Y., and Ohira, H. (2006) *J. Neuroimmunol.* **181**(1-2), 150-156
103. Oremek, G. M., Müller, R., Sapoutzis, N., and Wigand, R. (2003) *Anticancer Res.* **23**(2A), 1131-1134
104. Kato, H., Fukuda, T., Parkison, C., McPhie, P., and Cheng, S. Y. (1989) *Proc. Natl. Acad. Sci. USA* **86**(20), 7861-7865
105. Giallongo, A., Feo, S., Moore, R., Croce, C. M., and Showe, L. C. (1986) *Proc. Natl. Acad. Sci. USA* **83**(18), 6741-6745
106. Gracy, R. W. (1975) *Methods Enzymol.* **41**, 442-447

FOOTNOTES

Abbreviations used: 2DE, two-dimensional gel electrophoresis; 7-AAD, 7-amino actinomycin D; ACN, Acetonitrile; EnoA, α-enolase; FBS, fetal bovine serum (heat inactivated); FDR, false discovery rate; FITC, fluorescein isothiocyanate; G3P, glyceraldehyde 3-phosphate; GAPDH, glyceraldehyde 3–phosphate dehydrogenase; IAI, innate apoptotic immunity; iTRAQ, isobaric tagging for relative and absolute quantification; LC, liquid chromatography; MALDI, matrix assisted laser desorption / ionization; MFI, mean fluorescence intensity; MS, mass spectrometry; MS / MS, tandem mass spectrometry; PE, phycoerythrin; PEP, phosphoenolpyruvate; PGK, phosphoglycerate kinase; PI, propidium iodide; PK, pyruvate kinase; PMA, phorbol myristate acetate; PTM, post-translational modification; SLE, systemic

lupus erythematosis; SUPER, surface-exposed (during apoptotic cell death), ubiquitously-expressed, protease-sensitive, evolutionarily-conserved, and resident normally in viable cells; TEAB, triethylammonium bicarbonate buffer; TPI, triosephosphate isomerase

FIGURE LEGENDS

Figure 1: Apoptotic suppressive determinants are protease-sensitive and enriched in membrane vesicles. Apoptotic suppression of NFκB-dependent transcription was assessed with respect to NFκB-dependent luciferase activity in B2.1 reporter cells (13). **A)** Suppression of phorbol myristate acetate (PMA; 1.25 ng / ml)-induced NFκB-dependent luciferase activity by graded numbers (indicated as the target : responder ratio) of viable (green) or apoptotic (actinomycin D, 200 ng / ml; red) S49 murine T cells (solid bars) and targets that had been digested with trypsin (0.1%, 15 min., 37°C; open bars) was assessed. Trypsin was removed from targets by extensive washing and residual activity was quenched by incubation in 10% serum-containing medium. **B)** Human epithelial (HeLa) cell targets were left untreated or treated with actinomycin D. The suppressive activity of cells (solid bars; target : responder ratio = 8:1) and vesicles (solid bars; target : responder ratio = 30:1), prepared by incubation of untreated and treated cells in Vesiculation Buffer (see Experimental Procedures), was assessed independently, as in **A**.

Figure 2: Analysis of membrane vesicle proteins by Two-Dimensional Gel Electrophoresis. Comparative analysis of membrane vesicle preparations from viable and apoptotic HeLa cells by two-dimensional gel electrophoresis. Multiple gel spots corresponding to Pyruvate Kinase (blue), α-Enolase (magenta), and Triosephosphate Isomerase (green) are indicated. The increased abundance of protein spots among apoptotic (relative to viable) membrane vesicles is indicated by up-arrows. Details are listed below.

Pyruvate Kinase (predicted molecular weight = 58 kDa, pI = 7.96; ref. 104):

Spots	apparent M_r	apparent pI	ratio[1]
1, 1'	~58 kDa	~5.7	1.9
2, 2'	~58 kDa	~5.8	1.3
3, 3'	~48 kDa	~6.5	1.1

α-Enolase (predicted molecular weight = 47 kDa, pI = 7.01; ref. 105):

Spots	apparent M_r	apparent pI	ratio[1]
4, 4'	~48 kDa	~7.1	2.1
5, 5'	~48 kDa	~7.5	1.4

Triosephosphate Isomerase (predicted molecular weight = 31 kDa, pI = 5.65; ref. 106):

Spots	apparent M_r	apparent pI	ratio[1]
6, 6'	~31 kDa	~7.1	1.2
7, 7'	~26 kDa	~7.3	3.6

1. The ratio of normalized densitometric intensities of a spot in the apoptotic sample to the comparable viable spot was determined.

Figure 3: Relative abundance of apoptotic and viable membrane vesicle proteins determined by iTRAQ analysis. Compilation of the relative abundance of membrane vesicle proteins from apoptotic versus viable preparations ("Apoptotic /' Viable"), determined by iTRAQ analysis (see Supplemental Table I). The relative abundance of selected proteins is indicated. Proteins involved as enzymes in the glycolysis pathway (marked in red; see inset) are found to be over-represented. Other molecules identified as "plasminogen receptors" (see text; marked in green) are under-represented.

Figure 4: Functional categorization of over-represented proteins from apoptotic membrane vesicles. Functional categorization (gene ontology) of proteins found to be enriched among apoptotic membrane vesicles by iTRAQ analysis (see Table I). The two largest groups of proteins (26.8% each) are those characterized as membrane proteins and structural and cytoskeletal elements (marked in brown), and as catalytic proteins (marked in green). Proteins associated with the glycolytic pathway are the largest coherent cohort (9.0%) within either group. The next largest groups are proteins associated with macromolecular synthesis (especially translation) and processing and proteases (21.4%; shaded in violet), and molecular chaperones (12.5%; cross- hatched magenta area).

Figure 5: Detail of EnoA data from iTRAQ analysis. Over-representation of α-enolase ascertained from the consistent iTRAQ ratios obtained from all related precursor ions. Plot of reporter ion 114 (Viable 1) versus 116 (Apoptotic 1) intensities for all peptides (purple dots) identified in iTRAQ experiment. Yellow dots represent the iTRAQ signals derived from spectra matched to α-enolase (A1).

Figure 6: Cytofluorimetric analysis of externalization of glycolytic enzyme molecules. Murine splenocytes that had undergone apoptosis spontaneously in culture (12 hr.) and freshly isolated, viable splenocytes were analyzed cytofluorimetrically following staining with (**A**) FITC-conjugated polyclonal Goat anti- α-Enolase peptide IgG (Santa Cruz Biotechnology), (**B**) polyclonal Rabbit anti-GAPDH IgG (Abcam) and secondary FITC-conjugated Goat anti-Rabbit IgG (Santa Cruz Biotechnology), and (**C**) polyclonal Rabbit anti-Triosephosphate Isomerase IgG (Novus Biologicals) and secondary FITC-conjugated Goat anti-Rabbit IgG (Santa Cruz Biotechnology). Profiles shown are for apoptotic (solid green histogram) and viable (black, dashed line) cells stained with the specific FITC-conjugated reagents, and for apoptotic cells stained with the secondary antibody alone (gray, dotted line; the profile of viable cells is identical). Cells that had lost membrane integrity (PI$^+$, reduced forward- and expanded side-angle light scatter) were excluded from these analyses by electronic gating.

Figure 7: Quantification of glycolytic enzyme molecules externalization. Apoptotic cells (induced with actinomycin D) were analyzed cytofluorimetrically without (solid histogram) or following permeabilization (colored dashed line). **A**) HeLa cells were stained with mouse monoclonal anti- α-Enolase (L-27; Santa Cruz Biotechnology) and secondary PE-conjugated Rat monoclonal anti-mouse IgG$_1$ (BD Biosciences). The mean fluorescence intensity (MFI) of staining for non-permeabilized cells is 156.5; MFI for permeabilized cells is 307.3; MFI for staining with secondary antibody alone (black, solid line) is 10.0. We calculate the fraction of total cellular EnoA that was externalized in this experiment as 49%. The profile of staining of permeabilized viable HeLa cells (MFI = 319.5) was very similar to that of permeabilized apoptotic HeLa cells. **B**) DO11.10 cells were stained with mouse monoclonal anti GAPDH (Abcam) and secondary FITC-conjugated Rat anti-mouse IgG$_{2b}$ (BD Biosciences). MFI for non-permeabilized cells is 67.2; MFI for permeabilized cells is 142.0; MFI for staining with secondary antibody alone (black, solid line) is 15.2; the fraction of total cellular GAPDH externalized is 41%. The profile of staining of permeabilized viable DO11.10 cells (MFI = 138.5) was indistinguishable from that of permeabilized apoptotic DO11.10 cells.

Figure 8: Characterization of the appearance of exposed glycolytic enzyme molecules. Murine splenocytes that were induced to undergo apoptosis with staurosporine were analyzed cytofluorimetrically following staining with PE-conjugated annexin V, 7-AAD, and (**A**) FITC-conjugated polyclonal Goat anti- α-Enolase peptide IgG (Santa Cruz Biotechnology), (**B**) polyclonal Rabbit anti-GAPDH IgG (Abcam) and secondary FITC-conjugated Goat anti-Rabbit IgG (Santa Cruz Biotechnology), and (**C**) polyclonal Rabbit anti-Triosephosphate Isomerase IgG (Novus Biologicals) and secondary FITC-conjugated Goat anti-Rabbit IgG (Santa Cruz Biotechnology). Cells that met the criteria of staining positively with annexin V and negatively with 7-AAD (annexin V$^+$ 7-AAD$^-$; the "R1" region marked in red in the upper dot plots) were gated electronically, and the fluorescein signal of those cells was analyzed (shown as solid green histograms in the lower panels). The fluorescein signal of annexin V$^+$ 7-AAD$^-$ cells stained with secondary antibody alone also is presented (gray, dotted lines).

Figure 9: Cytofluorimetric analysis of plasminogen binding to apoptotic cells. **A**) Murine splenocytes that had undergone apoptosis spontaneously in culture (12 hr.) and freshly isolated, viable splenocytes were analyzed cytofluorimetrically as in Figure 6,following staining with FITC-conjugated plasminogen (BioMac). **B**) Murine splenocytes that were induced to undergo apoptosis with staurosporine were analyzed cytofluorimetrically following staining with PE-conjugated annexin V, 7-AAD, and FITC-conjugated plasminogen, and analyzed as in Figure 8.

Figure 10: Cytofluorimetric analysis of externalization of other molecules. Human transformed (Jurkat) T lymphocytes, that had been induced to undergo apoptosis by treatment with actinomycin D or had been left untreated, were analyzed cytofluorimetrically following staining with (**A**) FITC-conjugated mouse monoclonal anti-human Annexin-II (BD Biosciences) or (**B**) Mouse monoclonal anti-Calreticulin and secondary FITC-conjugated Goat anti-Rabbit IgG (Enzo Life Sciences). Apoptotic (solid green histogram) and viable (dashed line) cells were identified by scatter properties and gated electronically.

16

TABLES

Table I: Over-represented apoptotic membrane-associated proteins.

	Identified Proteins	Accession ID	Ratio	T-test
1	Cytochrome c	CYC_HUMAN	2.71	0.01
2	Stathmin	STMN1_HUMAN	2.07	0.00
3	Macrophage migration inhibitory factor	MIF_HUMAN	2.00	0.01
4	Acyl-CoA-binding protein	ACBP_HUMAN	1.94	0.05
5	SUMO-conjugating enzyme UBC9	UBC9_HUMAN	1.81	0.02
6	Profilin-1	PROF1_HUMAN	1.80	0.01
7	T-complex protein 1 subunit epsilon	TCPE_HUMAN	1.74	0.01
8	Peptidyl-prolyl cis-trans isomerase A	PPIA_HUMAN	1.74	0.00
9	Calpastatin	ICAL_HUMAN	1.68	0.03
10	Glutathione S-transferase omega-1	GSTO1_HUMAN	1.68	0.00
11	Aldose reductase	ALDR_HUMAN	1.68	0.02
12	Heat shock protein HSP 90-alpha	HS90A_HUMAN	1.68	0.05
13	Transgelin-2	TAGL2_HUMAN	1.68	0.05
14	Plastin-3	PLST_HUMAN	1.62	0.01
15	Nucleoside diphosphate kinase B	NDKB_HUMAN	1.62	0.03
16	14-3-3 protein beta/alpha	1433B_HUMAN	1.57	0.02
17	Thioredoxin	THIO_HUMAN	1.56	0.03
18	Myristoylated alanine-rich C-kinase substrate	MARCS_HUMAN	1.52	0.05
19	Importin-7	IPO7_HUMAN	1.52	0.01
20	Glutathione S-transferase P	GSTP1_HUMAN	1.51	0.02
21	Alpha-actinin-1	ACTN1_HUMAN	1.46	0.01
22	Spectrin beta chain, brain 1	SPTB2_HUMAN	1.46	0.01
23	Cytosolic phospholipase A2	PA24A_HUMAN	1.46	0.01
24	ATP synthase subunit d, mitochondrial	ATP5H_HUMAN	1.46	0.01
25	Nuclear migration protein nudC	NUDC_HUMAN	1.46	0.01
26	Alpha-enolase	ENOA_HUMAN	1.46	0.03
27	Fructose-bisphosphate aldolase A	ALDOA_HUMAN	1.46	0.03
28	T-complex protein 1 subunit theta	TCPQ_HUMAN	1.46	0.03
29	Phosphoglycerate kinase 1	PGK1_HUMAN	1.46	0.03
30	Heat shock cognate 71 kDa protein	HSP7C_HUMAN	1.37	0.01
31	Actin-related protein 2/3 complex subunit 3	ARPC3_HUMAN	1.37	0.01
32	Nascent polypeptide-associated complex subunit alpha	NACA_HUMAN	1.37	0.01
33	Superoxide dismutase [Cu-Zn]	SODC_HUMAN	1.36	0.05
34	Proteasome subunit beta type-3	PSB3_HUMAN	1.36	0.05
35	Triosephosphate isomerase	TPIS_HUMAN	1.36	0.05
36	Heat shock protein HSP 90-beta	HS90B_HUMAN	1.36	0.05
37	14-3-3 protein epsilon	1433E_HUMAN	1.36	0.05
38	Tyrosyl-tRNA synthetase, cytoplasmic	SYYC_HUMAN	1.36	0.05
39	Ubiquitin-like modifier-activating enzyme 1	UBA1_HUMAN	1.36	0.05
40	Ezrin	EZRI_HUMAN	1.32	0.03
41	Cofilin-1	COF1_HUMAN	1.32	0.03
42	Transgelin	TAGL_HUMAN	1.32	0.03
43	Proteasome subunit alpha type-5	PSA5_HUMAN	1.32	0.00
44	T-complex protein 1 subunit gamma	TCPG_HUMAN	1.32	0.04
45	L-lactate dehydrogenase A chain	LDHA_HUMAN	1.32	0.04
46	Ras-related protein Rab-1B	RAB1B_HUMAN	1.28	0.02
47	Actin-related protein 2/3 complex subunit 2	ARPC2_HUMAN	1.27	0.02
48	Eukaryotic peptide chain release factor GTP-binding subunit ERF3A	ERF3A_HUMAN	1.27	0.02
49	Fatty acid synthase	FAS_HUMAN	1.23	0.00
50	Protein SET	SET_HUMAN	1.19	0.04

17

	Identified Proteins	Accession ID	Ratio	T-test
51	Phosphoglycerate mutase 1	PGAM1_HUMAN	1.19	0.04
52	Elongation factor 1-gamma	EF1G_HUMAN	1.19	0.04
53	Proliferation-associated protein 2G4	PA2G4_HUMAN	1.19	0.03
54	Elongation factor 2	EF2_HUMAN	1.19	0.03
55	Acidic leucine-rich nuclear phosphoprotein 32 family member A	AN32A_HUMAN	1.19	0.03
56	Importin subunit beta-1	IMB1_HUMAN	1.19	0.03

Proteins identified by iTRAQ analysis and found to be over- represented among apoptotic membrane vesicles by at least 20% at a confidence level greater than 95% are listed.

Table II: Under-represented apoptotic membrane-associated proteins.

	Identified Proteins	Accession ID	Ratio	T-test
1	Histone H2A type 2-B	H2A2B_HUMAN	0.28	0.01
2	Large neutral amino acids transporter small subunit 1	LAT1_HUMAN	0.29	0.03
3	Dipeptidyl peptidase 1	CATC_HUMAN	0.31	0.02
4	Small nuclear ribonucleoprotein-associated proteins B and B'	RSMB_HUMAN	0.32	0.03
5	Alkaline phosphatase, tissue-nonspecific isozyme	PPBT_HUMAN	0.42	0.03
6	Asparagine synthetase [glutamine-hydrolyzing]	ASNS_HUMAN	0.42	0.02
7	60S ribosomal protein L19	RL19_HUMAN	0.45	0.03
8	Annexin A5	ANXA5_HUMAN	0.45	0.02
9	Annexin A6	ANXA6_HUMAN	0.47	0.02
10	60S ribosomal protein L24	RL24_HUMAN	0.50	0.02
11	Cytochrome b-c1 complex subunit 7	QCR7_HUMAN	0.50	0.02
12	40S ribosomal protein S17	RS17_HUMAN	0.52	0.00
13	Keratin, type I cytoskeletal 10	K1C10_HUMAN	0.54	0.04
14	60S ribosomal protein L34	RL34_HUMAN	0.56	0.04
15	40S ribosomal protein S2	RS2_HUMAN	0.57	0.03
16	Annexin A2	ANXA2_HUMAN	0.57	0.03
17	Heat shock protein beta-1	HSPB1_HUMAN	0.57	0.00
18	40S ribosomal protein S23	RS23_HUMAN	0.57	0.01
19	Protein S100-A4	S10A4_HUMAN	0.57	0.03
20	60S ribosomal protein L32	RL32_HUMAN	0.58	0.01
21	Programmed cell death protein 6	PDCD6_HUMAN	0.59	0.03
22	60S ribosomal protein L36a	RL36A_HUMAN	0.59	0.00
23	DNA replication licensing factor MCM5	MCM5_HUMAN	0.60	0.02
24	60S ribosomal protein L9	RL9_HUMAN	0.60	0.02
25	Protein transport protein Sec31A	SC31A_HUMAN	0.60	0.02
26	Tubulin beta-4 chain	TBB4_HUMAN	0.60	0.05
27	Protein S100-A10	S10AA_HUMAN	0.61	0.03
28	Small nuclear ribonucleoprotein Sm D3	SMD3_HUMAN	0.61	0.03
29	Polypeptide N-acetylgalactosaminyltransferase 2	GALT2_HUMAN	0.62	0.00
30	Non-POU domain-containing octamer-binding protein	NONO_HUMAN	0.62	0.01
31	60S ribosomal protein L14	RL14_HUMAN	0.62	0.04
32	Endothelin-converting enzyme 1	ECE1_HUMAN	0.62	0.04
33	Keratin, type II cytoskeletal 8	K2C8_HUMAN	0.64	0.04
34	Interleukin enhancer-binding factor 3	ILF3_HUMAN	0.64	0.04
35	Histone H2B type 1-J	H2B1J_HUMAN	0.64	0.01
36	DNA replication licensing factor MCM4	MCM4_HUMAN	0.64	0.02
37	Histone H1.5	H15_HUMAN	0.64	0.02
38	40S ribosomal protein S18	RS18_HUMAN	0.66	0.04
39	Annexin A1	ANXA1_HUMAN	0.66	0.04
40	60S ribosomal protein L26	RL26_HUMAN	0.66	0.00
41	Lysosome-associated membrane glycoprotein 1	LAMP1_HUMAN	0.66	0.01
42	Delta(3,5)-Delta(2,4)-dienoyl-CoA isomerase, mitochondrial	ECH1_HUMAN	0.66	0.01

18

43	Splicing factor, arginine/serine-rich 6	SFRS6_HUMAN	0.66	0.01
44	Mitochondrial carrier homolog 2	MTCH2_HUMAN	0.66	0.01
45	Probable ATP-dependent RNA helicase DDX17	DDX17_HUMAN	0.66	0.01
46	40S ribosomal protein S16	RS16_HUMAN	0.68	0.05
47	40S ribosomal protein S3a	RS3A_HUMAN	0.68	0.05
48	Clathrin light chain A	CLCA_HUMAN	0.68	0.05
49	EGF-like repeat and discoidin I-like domain-containing protein 3	EDIL3_HUMAN	0.68	0.05
50	Guanine nucleotide-binding protein G(I)/G(S)/G(T) subunit beta-1	GBB1_HUMAN	0.68	0.05
51	40S ribosomal protein S9	RS9_HUMAN	0.68	0.01
52	N-acetylgalactosaminyltransferase 7	GALT7_HUMAN	0.68	0.01
53	40S ribosomal protein S15a	RS15A_HUMAN	0.68	0.01
54	Aspartyl-tRNA synthetase, cytoplasmic	SYDC_HUMAN	0.68	0.01
55	X-ray repair cross-complementing protein 5	XRCC5_HUMAN	0.68	0.03
56	Interleukin enhancer-binding factor 2	ILF2_HUMAN	0.68	0.03
57	Protein ERGIC-53	LMAN1_HUMAN	0.69	0.05
58	60S ribosomal protein L23	RL23_HUMAN	0.71	0.05
59	Heterogeneous nuclear ribonucleoproteins A2/B1	ROA2_HUMAN	0.71	0.00
60	Peroxiredoxin-2	PRDX2_HUMAN	0.71	0.00
61	60S ribosomal protein L13	RL13_HUMAN	0.71	0.02
62	Reticulon-4	RTN4_HUMAN	0.71	0.02
63	60S ribosomal protein L18	RL18_HUMAN	0.71	0.02
64	60S ribosomal protein L15	RL15_HUMAN	0.71	0.03
65	Myosin light polypeptide 6	MYL6_HUMAN	0.73	0.02
66	60S ribosomal protein L6	RL6_HUMAN	0.73	0.02
67	Heterogeneous nuclear ribonucleoproteins C1/C2	HNRPC_HUMAN	0.73	0.02
68	60S ribosomal protein L35	RL35_HUMAN	0.73	0.01
69	Calumenin	CALU_HUMAN	0.73	0.01
70	DNA topoisomerase 2-alpha	TOP2A_HUMAN	0.73	0.01
71	Heterogeneous nuclear ribonucleoprotein G	HNRPG_HUMAN	0.73	0.01
72	60S ribosomal protein L3	RL3_HUMAN	0.73	0.05
73	ADP/ATP translocase 2	ADT2_HUMAN	0.73	0.05
74	Tubulin beta chain	TBB5_HUMAN	0.76	0.00
75	DNA-dependent protein kinase catalytic subunit	PRKDC_HUMAN	0.76	0.03
76	40S ribosomal protein S10	RS10_HUMAN	0.76	0.03
77	Vigilin	VIGLN_HUMAN	0.76	0.03
78	60S ribosomal protein L4	RL4_HUMAN	0.78	0.02
79	40S ribosomal protein S19	RS19_HUMAN	0.78	0.02
80	60S ribosomal protein L10	RL10_HUMAN	0.78	0.02
81	60S ribosomal protein L21	RL21_HUMAN	0.78	0.02
82	60S ribosomal protein L7a	RL7A_HUMAN	0.78	0.02
83	Heterogeneous nuclear ribonucleoprotein D0	HNRPD_HUMAN	0.78	0.02
84	Heterogeneous nuclear ribonucleoprotein R	HNRPR_HUMAN	0.78	0.02
85	40S ribosomal protein S4, X isoform	RS4X_HUMAN	0.81	0.05
86	60S ribosomal protein L13a	RL13A_HUMAN	0.81	0.05
87	60S ribosomal protein L23a	RL23A_HUMAN	0.81	0.05
88	60S ribosomal protein L18a	RL18A_HUMAN	0.81	0.05
89	Heterogeneous nuclear ribonucleoprotein L	HNRPL_HUMAN	0.81	0.05
90	Serpin H1	SERPH_HUMAN	0.81	0.05
91	Thymidylate kinase	KTHY_HUMAN	0.81	0.05
92	Trifunctional enzyme subunit alpha, mitochondrial	ECHA_HUMAN	0.81	0.05
93	ATP-dependent RNA helicase A	DHX9_HUMAN	0.84	0.04
94	26S protease regulatory subunit 4	PRS4_HUMAN	0.84	0.04
95	60S acidic ribosomal protein P0	RLA0_HUMAN	0.84	0.04

96	Actin-related protein 2	ARP2_HUMAN	0.84	0.04
97	Cytochrome b5	CYB5_HUMAN	0.84	0.04
98	Filamin-A	FLNA_HUMAN	0.84	0.04
99	Nucleolin	NUCL_HUMAN	0.84	0.04
100	Signal recognition particle 9 kDa protein	SRP09_HUMAN	0.84	0.04
101	60S ribosomal protein L7	RL7_HUMAN	0.84	0.03
102	40S ribosomal protein S8	RS8_HUMAN	0.84	0.03
103	60S ribosomal protein L35a	RL35A_HUMAN	0.84	0.03
104	Histone H2A.V	H2AV_HUMAN	0.84	0.03
105	Splicing factor, proline- and glutamine-rich	SFPQ_HUMAN	0.84	0.03

Proteins identified by iTRAQ analysis and found to be under- represented among apoptotic membrane vesicles by at least 20% at a confidence level greater than 95% are listed.

Table III: Cell-associated Enzymatic Activities.

Enolase activity (HeLa cells) (conversion of 2 phosphoglycerate to phosphoenolpyruvate [PEP], nMol / 10^4 cells)		
	Cells from	
	Viable Populations	Apoptotic Populations
Disrupted cell activity	9.7 ± 1.1	3.7 ± 0.8
Undisrupted cell activity	1.9 ± 0.4	1.9 ± 0.5
Undisrupted cell supernatant activity	1.4 ± 0.2	1.2 ± 0.2

GAPDH activity (HeLa cells) (Glyceraldehyde 3-phosphate-dependent formation of NADH, nMol / 10^4 cells)		
	Cells from	
	Viable Populations	Apoptotic Populations
Disrupted cell activity	5.5 ± 0.8	3.4 ± 0.1
Undisrupted cell activity	0.8 ± 0.1	1.4 ± 0.4
Undisrupted cell supernatant activity	1.2 ± 0.3	1.2 ± 0.1

Enolase and GAPDH activities were assessed as described in Experimental Procedures. Graded numbers of undisrupted viable or apoptotic HeLa cells, or the sonicated extracts of equivalent cell numbers (disrupted cells), were incubated in 200 µl reactions for 4 min. at 25°C. Cells and cell debris then was removed by centrifugation, and reaction products were quantified spectrophotometrically. Activity in cell supernatants was assessed by incubating cells as above in mock reactions without substrate, removing cells by centrifugation, and then incubating supernatants with substrate for an additional 4 min. at 25°C.

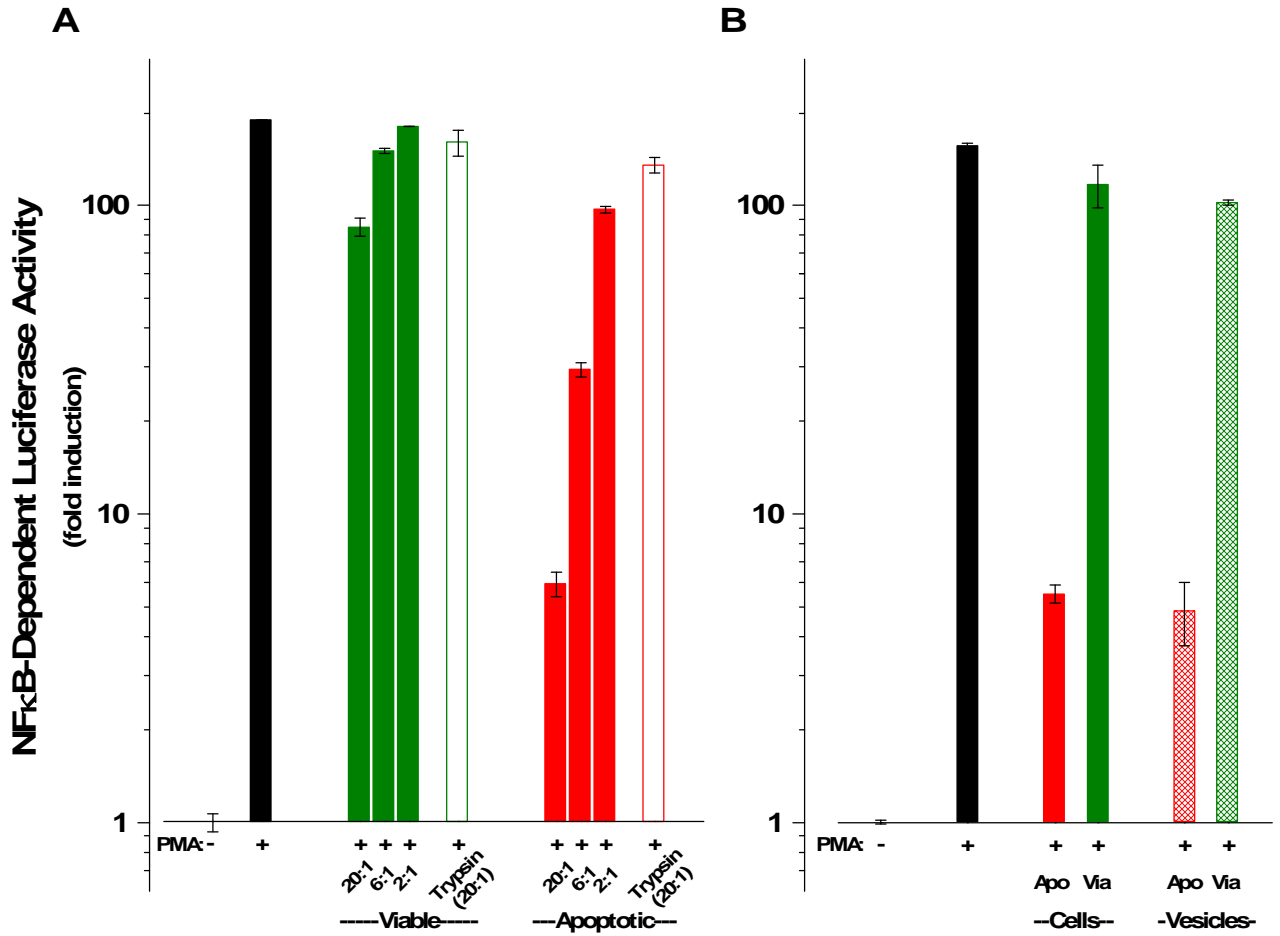**Figure 1: Apoptotic suppressive determinants are protease-sensitive and enriched in membrane vesicles**.

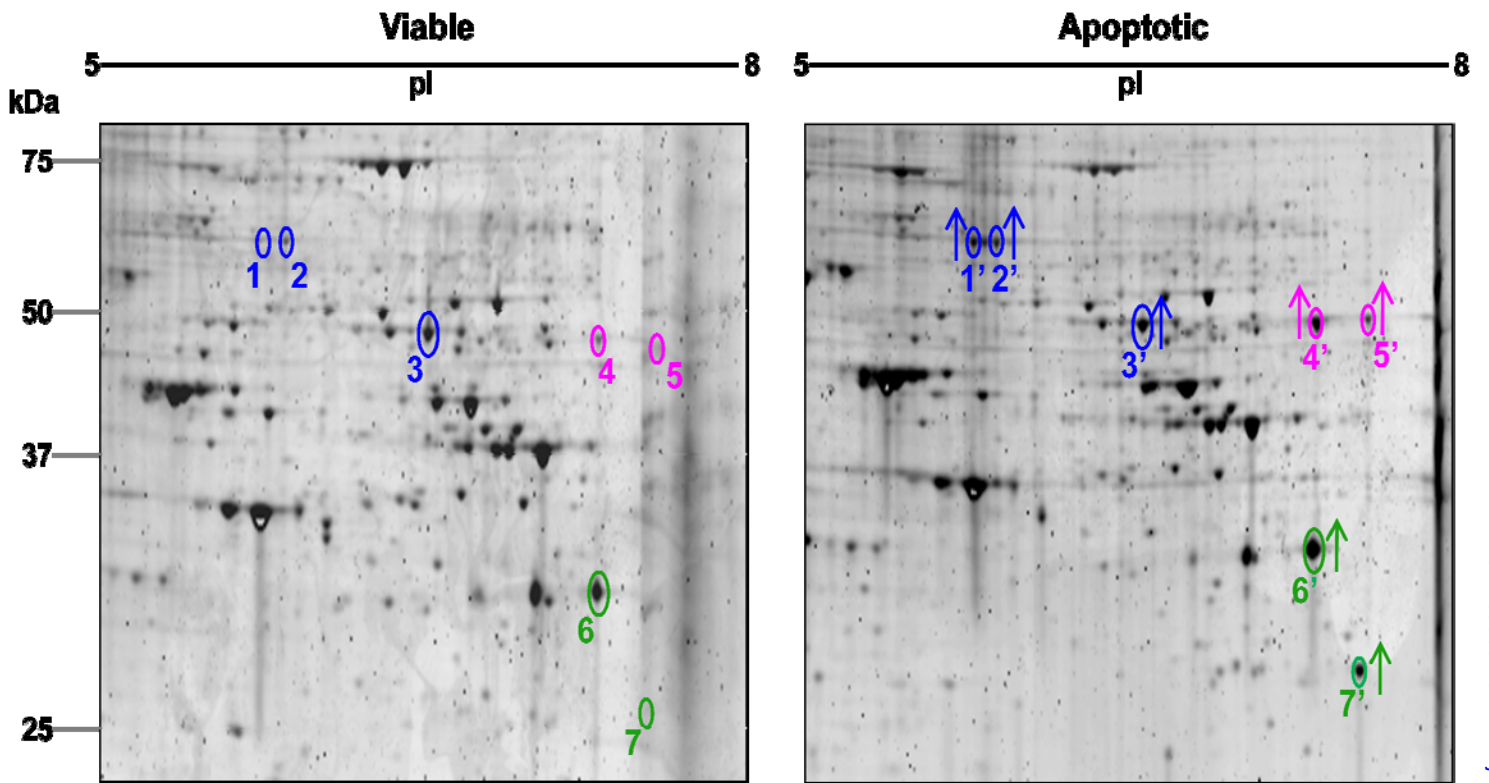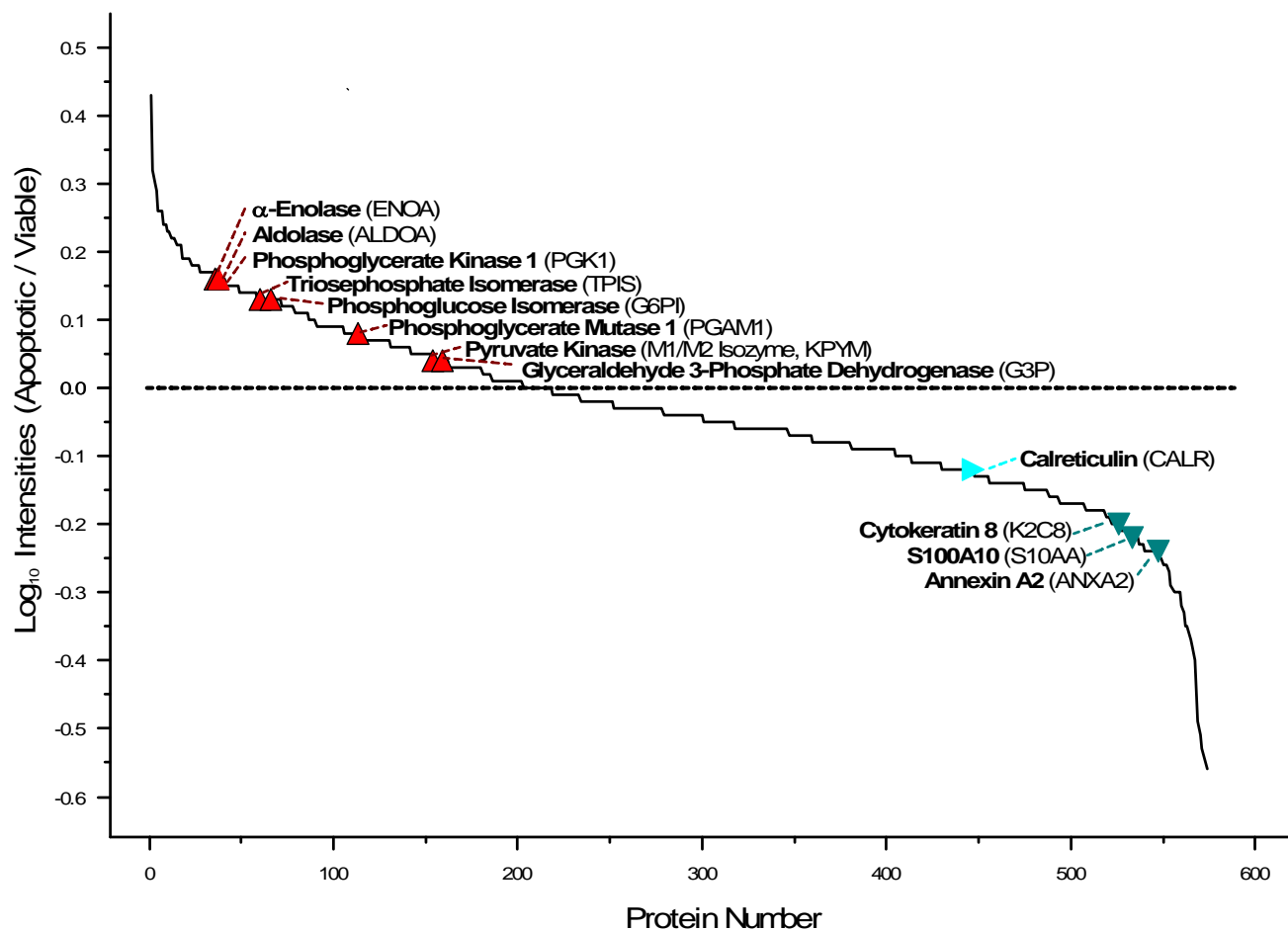**Figure 2: Analysis of membrane vesicle proteins by Two-Dimensional Gel Electrophoresis.**

Figure 3: **Relative abundance of apoptotic and viable membrane vesicle proteins determined by iTRAQ analysis.**
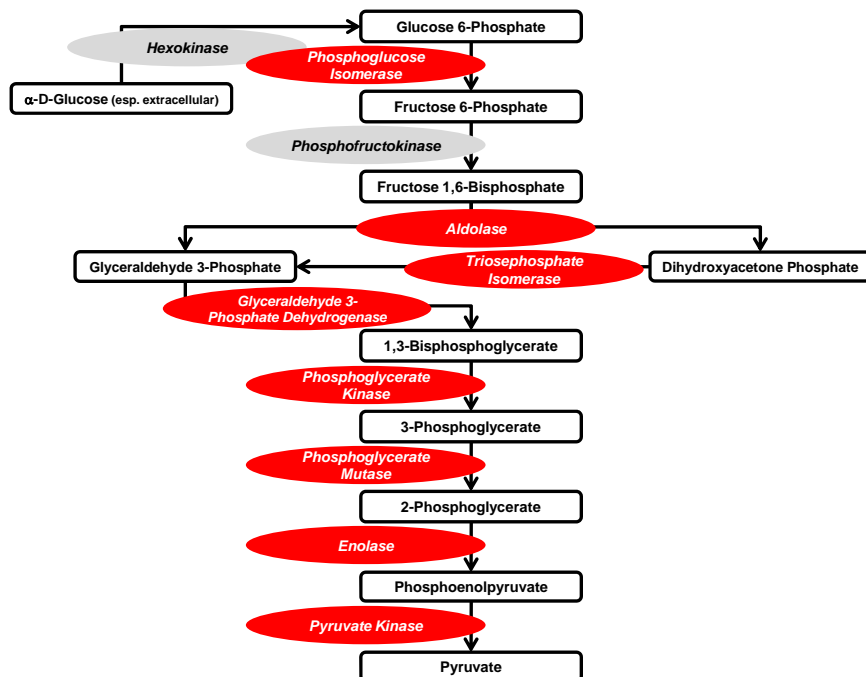
Insert: (Glycolytic pathway)

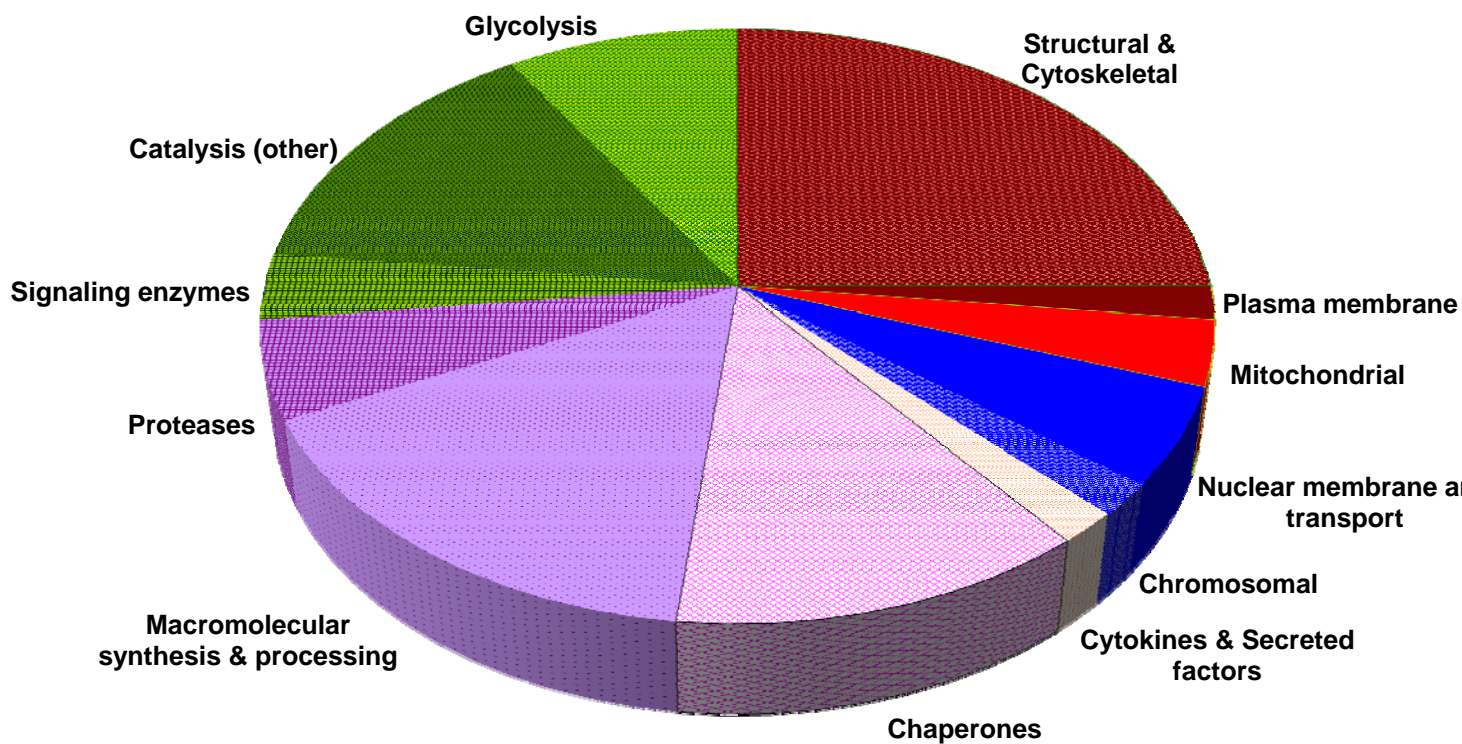**Figure 4: Functional categorization of over-represented proteins from apoptotic membrane vesicles.**
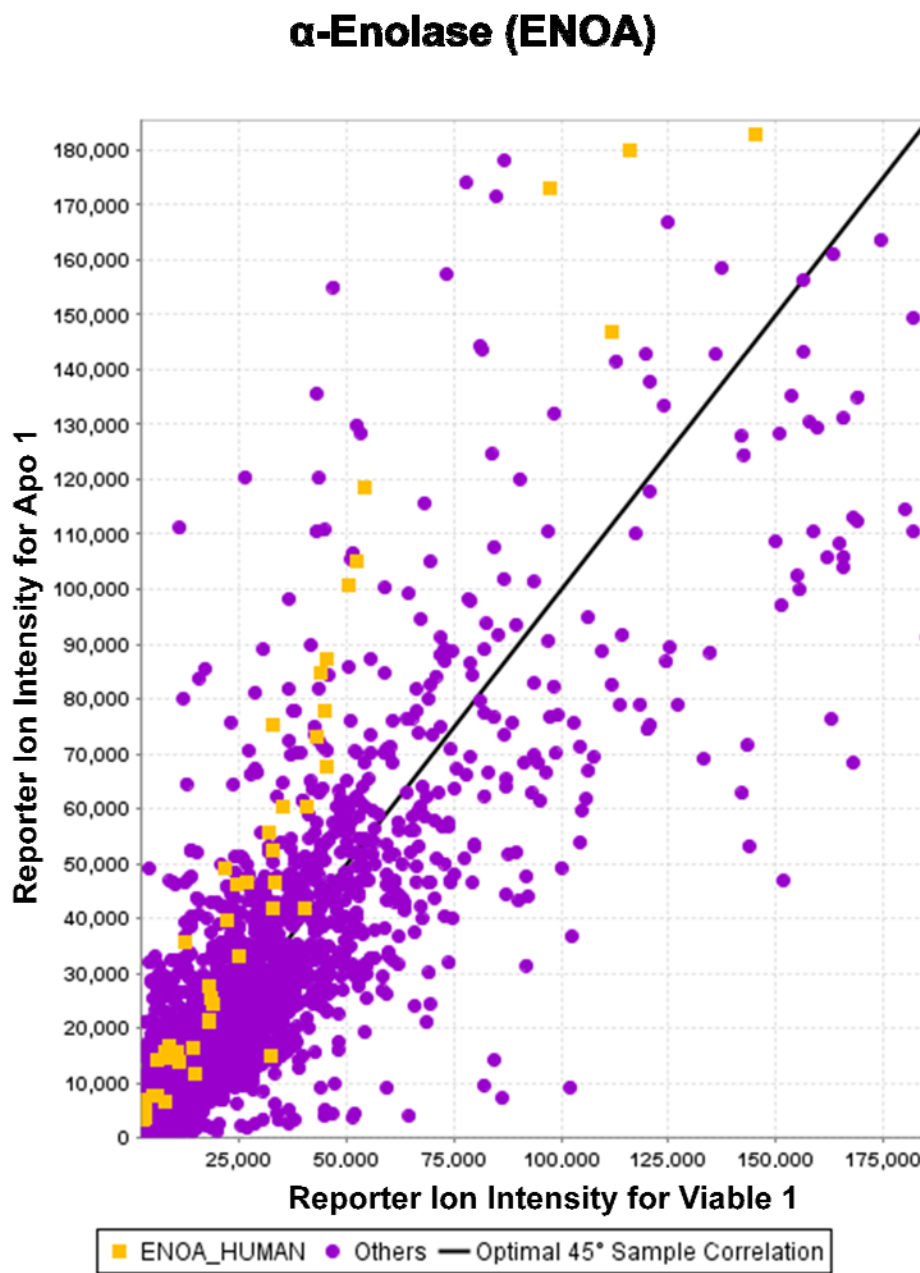
Figure 5: Detail of EnoA data from iTRAQ analysis.

α-Enolase (ENOA)

Figure 6: Cytofluorimetric analysis of externalization of glycolytic enzyme molecules.

A. α-Enolase **B.** Glyceraldehyde 3-Phosphate Dehydrogenase (GAPDH) **C.** Triosephosphate Isomerase (TPI)
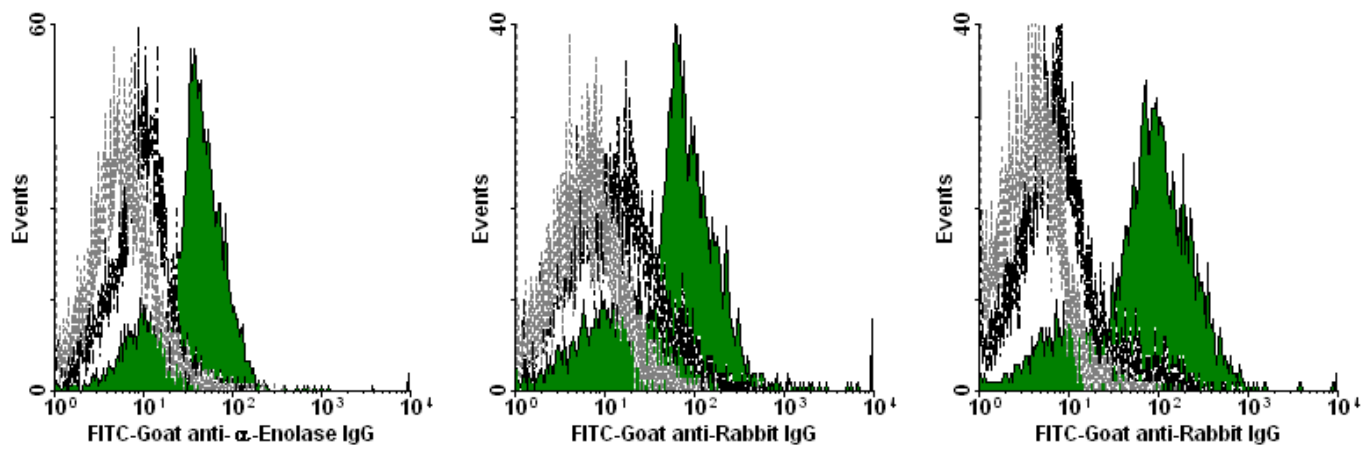
Figure 7: Quantification of glycolytic enzyme molecules externalization.
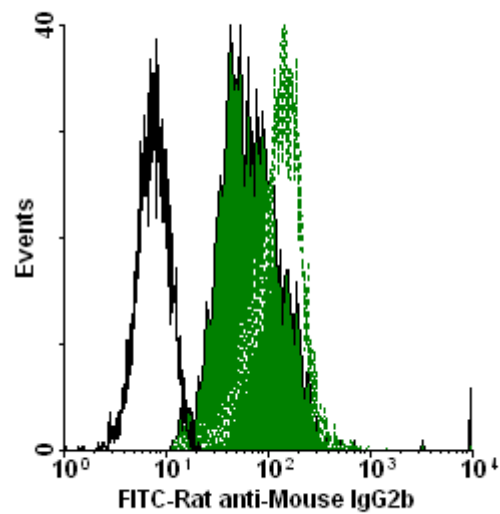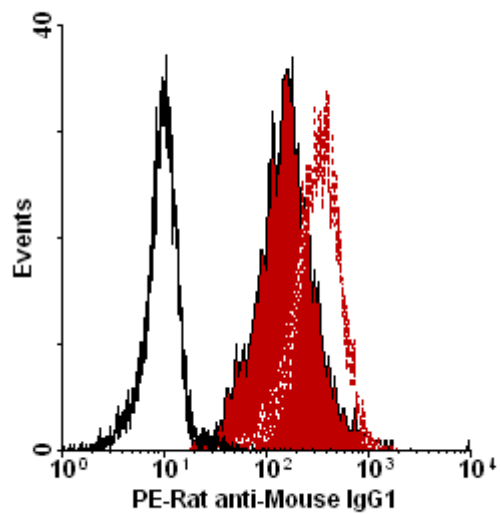
A. α-Enolase   **B.** GAPDH

Figure 8: Characterization of the appearance of exposed glycolytic enzyme molecules.

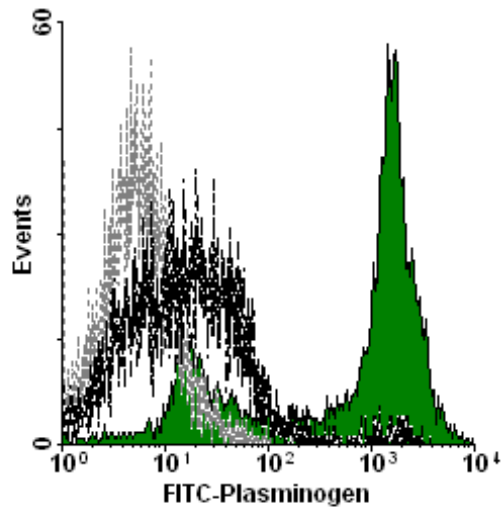**A.** α-Enolase   **B.** GAPDH   **C.** TPI

28
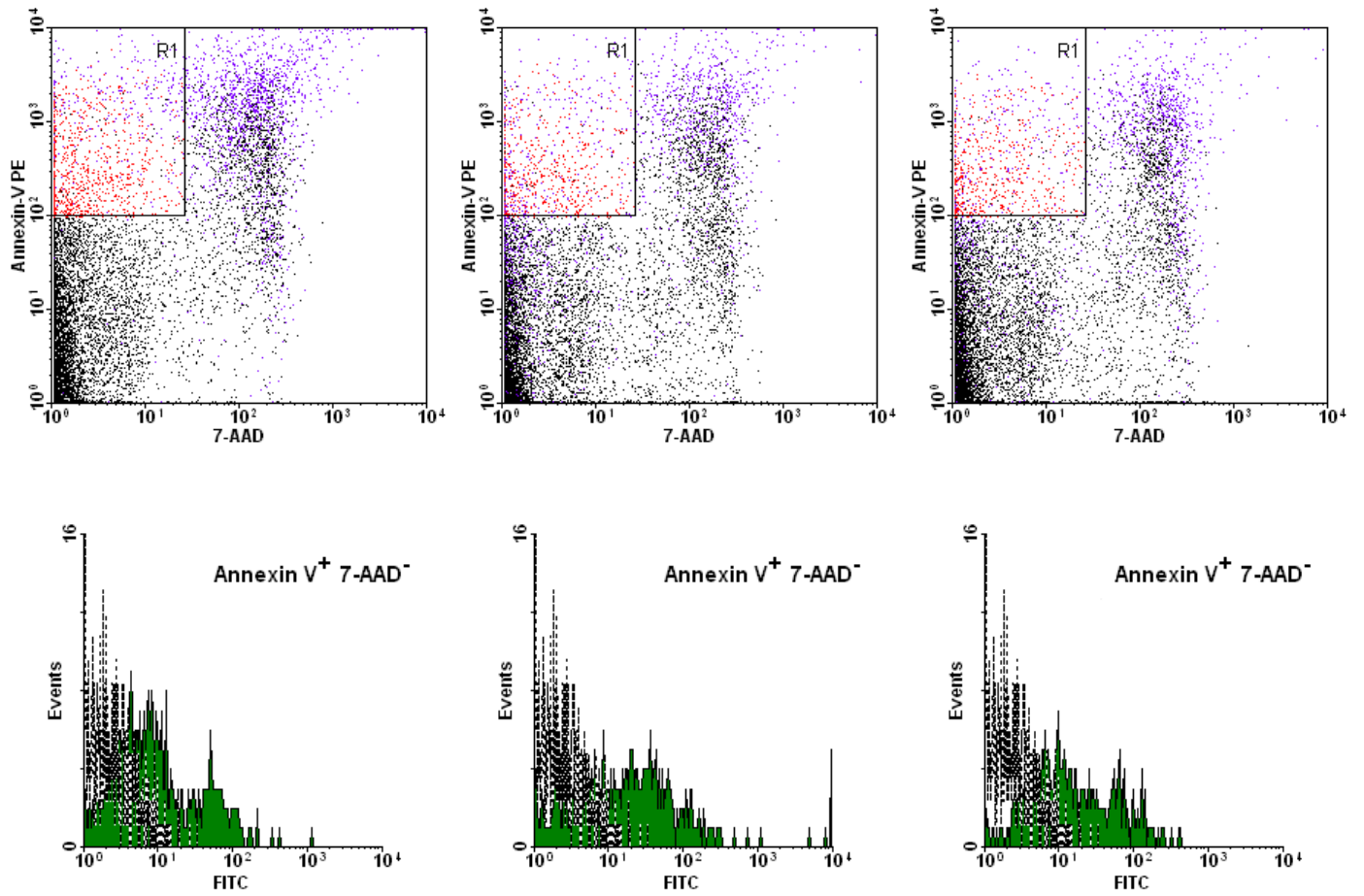
Figure 9: Cytofluorimetric analysis of plasminogen binding to apoptotic cells.
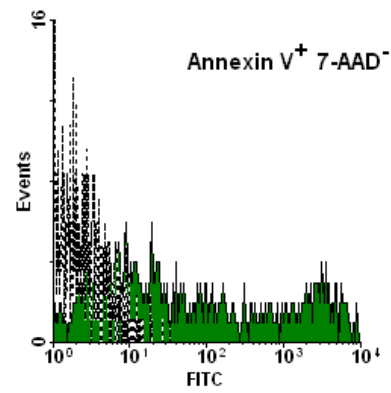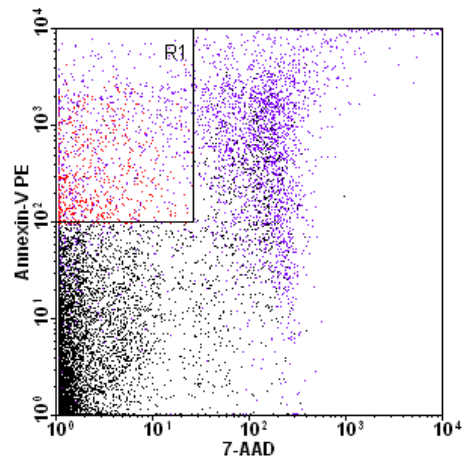
A.

B.

Figure 10: Cytofluorimetric analysis of externalization of other molecules.

A. Annexin A2

B. Calreticulin